KERNFORSCHUNGSZENTRUM

KARLSRUHE

September 1970

KFK 1266
EUR 3969 e

Institut für Angewandte Reaktorphysik
Institut für Neutronenphysik und Reaktortechnik
Projekt Schneller Brüter

Physics Investigations of Steam-Cooled Fast Reactor Cores with a Plutonium-Fueled Central Zone. SNEAK-Assembly 3B

Compiled by
E.A. Fischer, F. Helm, H. Werle

GESELLSCHAFT FÜR KERNFORSCHUNG M.B.H.
KARLSRUHE

KERNFORSCHUNGSZENTRUM KARLSRUHE

September 1970

KFK 1266

EUR 3969e

Institut für Angewandte Reaktorphysik

Institut für Neutronenphysik und Reaktortechnik

Projekt Schneller Brüter

Physics Investigations of Steam-Cooled Fast Reactor Cores with a Plutonium-Fueled Central Zone. SNEAK-Assembly 3B[1]

Compiled by

E.A. Fischer, F. Helm, and H. Werle

With contributions from

L. Barleon, W. Bickel, H. Bluhm, R. Böhme, K. Böhnel, R. Buyl[2], U. Däunert, M. Edelmann, P. Engelmann, G. Fieg, G. Günther, F.W.A. Habermann[2], D. Kuhn, M. Müller, W.J. Oosterkamp, A.M. Raberain[2], R. Schröder, P.L. van Velze[2], H. Walze, G. Wittek, J. Woite

1. Work performed within the association in the field of fast reactors between the European Atomic Energy Community and Gesellschaft für Kernforschung mbH., Karlsruhe

2. EURATOM

Gesellschaft für Kernforschung mbH., Karlsruhe

Abstract

In SNEAK Assembly 3B the physics parameters of a steam-cooled fast reactor core were investigated, the steam being simulated by polyethylene foils. The core had a central zone fuelled with plutonium and a surrounding uranium zone. It was also modified by introducing nickel and molybdenum for the simulation of Inconel and by introducing platelets containing a mock-up of fission products.

The experiments were compared to calculations, often using various nuclear data sets or calculational methods.

The work reported here is a direct continuation of the experiments in a uranium fuelled steam-cooled fast reactor core SNEAK 3A described in the KFK-reports Nr. 627 and 847.

Zusammenfassung

In der Anordnung SNEAK 3B wurden physikalische Untersuchungen über ein dampfgekühltes schnelles Reaktor-Core durchgeführt, wobei der Dampf durch Polyäthylen-Folien simuliert wurde. Das Core hatte eine zentrale Zone mit Plutoniumbrennstoff, die von einer Uranzone umgeben war. Es wurde modifiziert durch das Einbringen von Nickel und Molybdän zur Simulation von Inconel und durch das Einbringen von Plättchen mit Spaltproduktersatzgemisch.

Die experimentellen Ergebnisse wurden mit Rechnungen verglichen, wobei oft verschiedene Kerndatensätze und Berechnungsmethoden verwendet wurden.

Die Arbeiten, über die hier berichtet wird, sind eine direkte Fortsetzung der Experimente in der dampfgekühlten schnellen Urananordnung SNEAK 3A, die in den KFK-Berichten Nr. 627 und 847 beschrieben wurde.

1. Introduction

The investigation on steam-cooled fast cores in SNEAK comprised a series of purely uranium-fuelled assemblies (SNEAK-3A /1,2/) and a second series of experiments performed with a central plutonium-fuelled zone of 29.9 cm radius, SNEAK-3B which is covered in this report. The experiments for SNEAK-3B were performed between March and August 1968. As in the preceding assemblies the steam-coolant was simulated by polyethylene foils. The plutonium fuel was introduced in the form of platelets containing a mixed oxide (25 % PuO_2, 75 % UO_2) canned by stainless steel. The composition of the central zone was chosen so as to have approximately the same material buckling and the same atomic densities of all non-fissionable materials as the uranium-fuelled composition of SNEAK-3A2 which was maintained in the outer core zone.

Experiments were performed in three variations of the core.

1.) The basic assembly SNEAK-3B2

2.) A modification of the basic assembly in which part of the steel was replaced by Nickel and Molybdenum up to a radius of 20.59 cm. This assembly served to study the influence of Inconel as a structural material and was called 3B2 - Inconel.

3.) In a second modification in the whole plutonium zone platelets were introduced which were designed to simulate the effects of fission products. This assembly is designated 3B-2S.

The number "2" which appears in all three core designations refers as in the case of the preceding uranium cores to normal operating hydrogen density. In the case of voided or flooded configurations it is replaced by

0 for a voided composition (zero hydrogen density)
1 for partial voiding (40% of normal hydrogen density)
and 3 for a flooded composition (doubled hydrogen density)

In all cases the changes of the hydrogen density were introduced only in a small central zone of the core.

2. Description of the Cores

The outlines of the cores of the series SNEAK-3B are shown in Fig. 1-3. All cores have a height of 8o.4 cm, a radius of the central plutonium zone of 29.9 cm and a total volume in the vicinity of 500 l. In order to avoid spectral perturbation as far as possible the plutonium zone was kept free of shim and safety rods which are fuelled with uranium. The axial and radial blanket consist of depleted uranium and have thicknesses of approximately 3o and 35 cm, respectively.

Fig. 4 and 5 show the unit cells used in the core. The basic cell of the plutonium zone had to be more complicated than the unit cell in the central zone of SNEAK-3A in order to match material buckling and atomic densities of non-fissionable isotopes of the uranium zone. In order to introduce molybdenum and nickel in realistic quantities for the Inconel simulation the cell height had to be doubled.

The development of the fission product simulation is described in /3/. Two versions of mock-fission product platelets were used in assembly 3B2-S. One version contains the expensive elements Ru, Rh and Pd (SPE II) while in the other these elements were replaced by an approximate neutronic equivalent of neodymium and silver (SPE I).
There were available about 2000 platelets of SPE I but only loo platelets of the expensive SPE II. The latter was used in the center of the plutonium zone, or, more exactly in the 5 axially central cells of the 20 central elements.

The contents of the fission product mock-up platelets is shown in Table 1.

The uranium zone was for all assemblies essentially left as it was in the preceding core SNEAK-3A2. It therefore still contains the two different types of uranium cells (the simple 4-platelet cell in an inner, the more complicated cell in an outer region) which had to be used in 3A2, because of material restrictions. The atomic densities of all compositions used in SNEAK-3B are given in Table 2.

3. The Substitution Experiments

3.1 The reloading from SNEAK-3A2 (uranium core) to SNEAK-3B2, that is the insertion of the central plutonium fuelled zone was performed as a substitution experiment. This consists essentially in the stepwise replacement of an increasing number of uranium elements by plutonium elements starting from the central axis of the core. It is continued until the final size of the plutonium zone is reached.
From the changes in reactivity or critical radius introduced by each step one can derive the material buckling or the critical radius of a core consisting entirely of Pu-elements. Similarly the Inconel zone was introduced by progressive substitution. The application of the substitution method in fast critical facilities was first proposed by French scientists at Cadarache /4,5/. A detailed description of the method and its application was given in /6/, where also the substitution experiments made in SNEAK-3 are analyzed. A summary of the results is given in Table 3.

3.2 Complementary Experiments

1.) Small-zone substitution at variable locations.

In an attempt at a more accurate determination of the difference $\frac{\Delta D}{D}$ of the diffusion coefficients of two medii substitution of small zones or of single elements were performed in excentrical positions and the resulting reactivity changes were compared to the effect of equally sized zones in the core center. At the start of the Pu- for -U substitution the reactivity changes caused by substituting a central and a non-central Pu-element were compared. After the central Pu-zone reached its final size the reactivity effect was measured for a central and a non-central U-element and for a small uranium zone of 10 cm height in the central 9 elements of different vertical displacements.

Similar experiments were performed before and after the Inconel substitution. The geometrical details and the results are given in Table 4.

A calculational evaluation of the complementary experiments proved to be very difficult. In the Pu-for-U substitution the results are determined mostly by the boundary effect, as evidenced by the fact that both a substitution of a Pu-element in a U-zone and of a U element in a Pu-zone yield positive reactivity changes. In the Inconel substitution the boundary effect is of minor importance. However, it was not found possible to extract a consistent value for $\frac{\Delta D}{D}$ from the data.

4. k_{eff} Calculations

For the critical configuration of each assembly k_{eff} was calculated by 26 group diffusion theory with a number of different nuclear data sets. In general, the calculations were performed in one-dimensional cylindrical geometry. In order to describe transverse leakage as well as possible each assembly was calculated at least for one cross section set by the TDS code which performs a series of alternating axial and radial calculations, thus providing a realistic set of group dependend bucklings. The following cross section sets were used:

The original and the final version of the KFK-SNEAK set for steam-cooled fast reactors. These cross section sets are documented in / 7/and/8/, respectively. The differences between the two sets are only minor, they are due mostly to a recalculation of the resonance self-shielding factors.

The SNEAK-PMB set. Here the data of the KFK-SNEAK set were modified by lowering the U^{235}-fission and the U238-capture cross section in the 100 keV region according to the measurements by Pönitz, Menlove and Beckurts /9/.

The SNEAK-PMB-α set. It is identical with the SNEAK-PMB set except for the capture cross section of Pu^{239} at low energies where it was changed to correspond to the Pu-α data as recommended by Schomberg /10/.

The MOXTOT set.This is the most recently developed cross section set at Karlsruhe. Its derivation is described in detail in / 11 /. The most important modifications to the SNEAK-set data are: Pu-$_\alpha$ data according to measurements by Gwin, a revised inelastic scattering matrix and the MOXON data for U^{238} capture between 0.5 and 100 keV.

Finally, the Russian ABN set / 12 / was used. The data of this set for the less important isotopes were incorporated in the Karlsruhe SNEAK set.

Heterogeneity corrections were determined using cross sections found by cell calculations with the ZERA code / 13 /. This code is based on collision probability theory and allows to determine cell averaged cross sections for the actual configuration of the cell as well as for a pseudo-homogenized medium in which all plate thicknesses are reduced by a large factor (10^3 or 10^4). The difference in k_{eff} for these two sets was found by perturbation calculations. It indicates the influence of the heterogeneity on the multiplication constant. Heterogeneity calculations were performed with the original version of the KFK-SNEAK set only. The corrections found are assumed to apply equally to the calculations with other cross section sets.

Table 5 shows the results of the k_{eff} calculations, including some values for the uranium assemblies 3A1 and 3A2. The calculated heterogeneity correction is not included in the k_{eff}-values given, but is indicated in a separate column. A general survey of Table 5 yields the following results:

The SNEAK set is always underreactive and becomes more so as the hydrogen concentration increases and as plutonium is introduced into the core. Using the PMB data this tendency is reduced.

Introducing the Pu-α values of Schomberg yields considerably too low values for the k_{eff} of the Pu-assemblies. For the MOXTOT set this discrepancy is largely eliminated by the use of the lower Pu-α data by Gwin and of lower capture cross sections for U^{238}. As Table 5 shows, MOXTOT tends to overestimate the reactivity of uranium assemblies and still underestimates that of plutonium assemblies - remaining however, always within 2 % of the experimental value.

The introduction of simulated Inconel left the discrepancies between measurement and calculation essentially unchanged. The assembly poisoned with the mock-fission products was calculated more underreactive, indicating that the cross sections for these materials were not known very well.

The ABN set which was always found overreactive shows mostly the same trends as the SNEAK set. An exception is that the calculated k_{eff} is not decreased but rather increased when plutonium is introduced in place of uranium fuel. In all cases the heterogeneity corrections were not too significant compared with the still existing discrepancy between theory and experiment.

5. Traverses with Rhodium-, Gold- and Copper Foils.

The spectral transitions at the zone boudaries were investigated by activation traverses using foils of different spectral sensitivity. Gold and copper were activated as sandwich foils. This made it possible to determine the flux at the main resonances for these materials (577 eV vor Cu, 4.9 eV for Au). Thus, the measurement yielded a total of 5 traverses; the total activation for Rh, Cu and Au as well as the resonance activation for Cu and Au.

The main purpose of this experiment was to determine if the spectrum near the boundary of the two compositions can be synthesised linearly out of the equilibrium spectra of these compositons, as this is an assumption on which the theory of progressive substitution /4,5/ is based.

If one assumes that such a synthesis is possible at a certain point near the boundary the activation of a foil of type x in this point can be described by the equation

$$A_x(P) = a\, A_x(P_1) + b\, A_x(P_2) \qquad (1)$$

where P_1 and P_2 are points in the interior of the zones where the equilibrium spectrum prevails.

An equation of the same type can be written down for a foil of type y with a different spectral sensitivity. From the two equations and the measured activities the coefficients a and b can be calculated. If several pairs of different foil types yield the same coefficients a and b one may conclude that the flux in the point P is described with good accuracy by the equation

$$\phi\,(P) = a\,\phi(P_1) + b\,\phi\,(P_2) \qquad (2)$$

Radial traverses were measured after the Pu-composition was introduced up to a radius of 18.7 cm and after it had reached its final radius of 29.9 cm. Fig. 6 and 7 show the results for the coefficients a and b. In the case of the small plutonium zone (R_Z > 18.7 cm) the scatter of the coefficients for the different activation pairs is generally small between the points P_1 and P_2. For the completed plutonium zone (R_Z = 29.9 cm) the results are not as good, probably due to the fact that the outer reference point is too close to the core-blanket boundary and therefore is not representative for the equilibrium spectrum of the outer core zone.

Further information can be derived from this activation experiment by plotting the resonance activation of Cu and Au directly as a function of position and comparing it with calculated values for groups 15 and 21 of the SNEAK set which correspond to the energies of the main resonances for these two materials (Fig. 8 and 9). When normalized in the Pu-zone, the calculated values in the U-zone are too low, indicating that the evaluation overestimates the spectral differences. Improvements in the evaluation (corrections for higher resonances and heterogeneity) may reduce but most probably not eliminate the discrepancy.

6. Coolant Reactivity Coefficients

The void and flooding experiments in the SNEAK-3B cores were performed as in the case of the uranium core SNEAK-3A by removing all polyethylene out of the test region (void) or by doubling the reference concentration of SNEAK-3B2 (flooding). The reactivity effects were measured by restoring criticality with calibrated control rods. The experiments were performed in three regions: a small central region and two cylindrical regions extending axially through the whole core. The exact dimensions are given in Table 6.

The results of calculations and measurements are given in Tables 7 and 8. Again, for easier reference some data for the assemblies 3A1 and 3A2 were included.

The calculations were performed in one-dimensional diffusion theory using the (original) SNEAK set. In most cases the cross sections were used once without heterogeneity corrections (NORM) and once averaged over the actual heterogeneous cell configuration by the ZERA code (HET).

The effect for the central region was generally calulated using perturbation theory in plate geometry, while for the regions extending axially throughout the core cylindrical k_{eff} calculations were made for the reference case and for the voided (or flooded) case. In this type of caculations a correction factor was applied to eliminate the contribution of the region corresponding to the axial reflector savings. For assemblies 3A-1 and 3B universal bucklings were used which were adapted to the actual flux distribution in the separated direction. In the case of assembly 3A-2 energy dependent bucklings were used, which had been found by previous diffusion calculations.

An intercomparison of the measured data shows that the reactivity effects in the plutonium fuelled cores are only in the order of one half of the corresponding effects in the uranium cores. This is probably due to an essentially flat energy dependence of the Pu fission cross section in the energy region of maximum flux where the U^{235} fission cross section increases with lethargy causing a corresponding increase in the adjoint flux. Further, it appears that while the effect in uranium cores is approximately linear in the hydrogen concentration (equal void and flooding effects) in the plutonium cores flooding causes 3o to 4o % more reactivity change than voiding.

For the uranium cores calculations with normal and heterogeneity corrected cross sections agree reasonably well with each other and with the experiments. In the case of plutonium, particularly for the Inconel and for the fission product poisoned core the NORM cross sections yield reactivity effects very much smaller than the measured ones while the heterogeneity corrected data still give quite good agreement. In all cases calculated the value given by the HET data was within 26 % of the measurement.

In general one should keep in mind that errors of the order of 10 % may have been introduced into the calculations by causes such as an incorrect choice of buckling, to which the calculated void and flooding effect is very sensitive, a wrong estimate of the influence of the

axial reflector savings when evaluating radial k_{eff} calculations, and finally minor errors which were still in the ZERA code when the heterogeneity corrected calculation for the 3A assemblies were made. The accuracy of the measurements was about 10^{-5} in $\Delta k/k$.

7. A Comparison of the Measured and Calculated Influence of Inconel and Mock-Fission Products on Reactivity and CH_2-Void Effects.

In Table 9 some results of reactivity measurements and void measurements are arranged so as to show directly the influence of Inconel and the mock fission products on the parameters in question.

For the criticality determinations the results are quite satisfactory for Inconel while in the case of the fission product mock-up there is a larger discrepancy between calculated and measured effect. Here the main factor of uncertainty is the moisture contents of the platelets. Although an estimated amount of humidity has already been taken into account by calculated correction, this may not be sufficient since the estimate is based on an H_2O determination in only 7 out of 1500 platelets. Nevertheless it is improbable that the H_2O contents is in reality 5 times larger than assumed which would be necessary to explain the measured effect.

For the case of the coolant void effect the influence of the presence of the mock-fission products is described quite well by the calculations. Here the effect of the humidity in the platelets cancels to a large extent, since it is present in the normal as well as in the voided configuration. However, for the void experiments the influence of the Inconel is not described correctly, but considerably overestimated. The reason for this is probably the strong heterogeneity of the cell. In particular the molybdenum is concentrated in one platelet appearing only about every 10 cm.

8. Neutron-Spectrum Measurements

Neutron spectrum measurements were performed using the Li^6-sandwich spectrometer, proton recoil proportional counters and resonance foil sandwiches. We tried, for the first time, to get an experimental spectrum over a large energy range without arbitrary normalization factors by determining the absolut efficiency of each method. This is a difficult problem, which is described separately for each method and the attempt was only partly successful.

8.1 Li^6F - Semiconductor Sandwich Spectrometer

The method and the electronic system used is described elsewhere /14/. It covers the energy region from 500 keV to 6.5 MeV and measurements were performed only in the central position of SNEAK 3B-2 .

The detecting foil is a layer of 157 $\mu g/cm^2$ Li^6F on a 15 $\mu g/cm^2$ Vyns-film. A Si-surface barrier detector with a sensitive area of 300 mm^2 was used. The background from gammas and (n,α)- or (n, p) - reactions in Si is decreased by setting a threshold to 1.2 MeV and the use of a fast-slow coincidence. The residual background from (n,α)-and (n,p)-reactions in Si is determined in a separate run, where the Li^6F- foil was replaced by a equivalent Li^7F-foil and then corrected for by subtracting the normalized background spectrum. The energy calibration is done with a weak U^{233}-α- source deposited on the Li^6F-foil. The energy resolution - around 240 keV for thermal neutrons- improves a little with increasing neutron energy. The reactor was run at 1 W and at this power level distortions due to gamma pile-up are negligible.

For the evaluation the geometrical efficiency for an isotropic flux calculated in /14/, the Li^6 (n,α) cross section from /15/ and the unfolding program reported in /16/ is used. The absolute efficiency is calculated from the geometrical efficiency and the number of Li^6-atoms on the foil, which relies on specifications of the manufacturer and on comparisons with Au-foils in a thermal neutron field, and is estimated to be correct within 5 %. The detector arrangement is shown in Fig. 10.

8.2 Proton - Recoil Proportional Counters

Measurements were performed in the energy range from 10 keV to 1.5 MeV. Hydrogen filled spherical counters (diameter 3.94 cm, filling pressure 1,2, and 4 atm) were used below 600 keV and above 400 keV a cylindrical counter (diameter 3.8 cm, length 9.5 cm). Below about 50 keV the γ-n-discrimination technique with an analog pulse height computer described by BENNETT /17/ was applied. Because the preamplifier was immediately connected to the detectors, there was, as is shown in Fig. 10, much void around the detectors and this may have remarkable effects on the measured spectrum.

The measured proton spectra are evaluated in two steps:
First the contribution of neutrons with energies above an upper limit is subtracted. Then the resultant spectrum is differentiated and multiplied with energy dependend wall-effect-correction factors. In this approximate method the wall-effects are not fully corrected for but it was estimated that the error is smaller than 5 % /18/.

Severe overloading of the electronic system occurs in the energy range where the γ-n-discrimination technique has to be applied. This may give rise to systematic errors in the low energy range and may explain the discrepancies with time-of-flight results at various SUAK-assemblies, where generally the proton-recoil measurements show fewer neutrons below about 30 keV /19/.

To determine the absolute efficiency one has to know the number of hydrogen atoms in the active volume of the counter. Because in spherical counters the dead volume is very small the error in the absolute efficiency is due to uncertainties in the filling pressure only, which are estimated to be about 3 %. For the cylindrical counter the error in the absolute efficiency is larger and may amount to 5 % due to uncertainties in the determination of the active volume.

The overall systematic error in the evaluated neutron spectrum is estimated to be below 15 % in the energy range above 50 keV.

8.3 Resonance Foil Sandwiches

Measurements were performed in the central position of all SNEAK 3B-2 configurations. A more detailed description of the measuring technique is given elsewhere /2,19/.

Eleven isotopes were used, with their main resonances ranging between 1.5 eV and 3 KeV. The sandwiches consist of three foils which are contained in a Cd-capsule. Cd itself is also used and in this case the sandwich consisted of five foils (including the Cd-capsule). The measured difference between the activity of the outer and inner foils is evaluated using the more recent published resonance data (including November 1969). The materials selected for the measurements together with their characteristic features are given in Table 10.

During the activation the sandwiches were located in both Al-platelets of the SNEAK 3B-2 cell (platelets no. 1 and 11 of the normal cell). Both values, corrected for heterogenity effects were averaged to get the final result.

In order to get from D, the measured difference in the counting rate between outer and inner foil, the flux ϕ_M at the main resonance, the following relation was applied

$$\phi_M = \frac{D}{\varepsilon} \quad \frac{P_M}{K_M}$$

ε contains the sensitivity of the gamma-counter and the atom density of the resonance absorber. K_M is the selfshielding of the main resonance, and P_M is the relative contribution of the main resonance to the total measured quantity D. P_M is calculated from the data of all resonances and an assumed neutron spectrum. In Table 11 the calculated values of P_M and the measured percentage differences R of the activity of outer and inner foil are given for the four assemblies investigated.

The absolute efficiencies of the sandwiches were determined with the Cd-foils. Cd has been chosen because it has a relatively simple decay scheme and because the resonance parameters are well known. The Cd-activity was measured absolutely by the 4π-β-γ-coincidence technique and from this absolute activity and resonance selfshielding calculations performed with the TRIX-1 program, the absolute flux at the main resonance was determined.

8.4 Results

The absolute flux values obtained with the sandwich foils and the proton-recoil counters are in reasonable agreement /Fig. 11, 12/ whereas the values of the Li^6-spectrometer are about a factor of two below the proton-recoil results. Thus, this first attempt of determining, with different techniques absolute flux values to obtain an experimental spectrum over a wide energy range, was only partially successful. This important problem will be investigated in the future.

The calculated and the combined measured spectrum were normalized to equal flux in the range of proton-recoil counters. The proton-recoil measurements show for all assemblies fewer neutrons below and more neutrons above 0.2 MeV as compared with the calculated spectra, although the discrepancies are comparable with the estimated experimental errors /Fig. 14/. In the energy range below 3 KeV measured with the sandwich foils, the measured and calculated energy dependence of the spectrum agrees, but the measured absolute values are lower, especially for the softer spectra /Fig. 11, 12/. This discrepancy may be due to errors in the absolute efficiencies of the sandwich foils and/or the proton-recoil counters. For the fission product core /Fig. 13/ the fluxes were not measured absolutely. Therefore the spectra measured with sandwich foils and proton-recoil counters are compared separately with the calculations.

Although the absolute values of the spectrum measured with the Li^6-spectrometer are much lower than those determined with the other methods, the slope of the measured and calculated spectra agrees rather well in the energy range between 0.8 and 6.5 MeV /Fig. 11/. Below 0.8 MeV there is a steep increase in the Li^6- Spectrum, an effect, which is neither seen in the proton-recoil results nor in the calculated spectrum and which has been observed also in measurements at other assemblies. It is strongly assumed, that this discrepancy is due to the fact, that the unfolding procedure works not satisfactorily in energy ranges where there are large variations in $Li^6(n,\alpha)$- cross sections, and this is the case below 0.8 MeV.

In general the agreement between calculated and measured spectra is remarkably improved especially in the range of proton-recoil counters /Fig. 14/ over older measurements at SNEAK3A-2 /2/. This may be due to several improvements which meanwhile were made on the experimental equipment, particularly in the γ-n-discrimination for proton recoil counters. However, for final conclusions of this type more confidence must be established interrelating the results of the different methods for spectrum measurements.

9. Reaction Rates

Absolute reaction rates per nucleus were measured by calibrated cylindrical and parallel plate fission chambers and by foil activation techniques at the core center as well as in axial and radial traverses.

9.1 Spectral Indices

The ratios of central fission rates of Th232, U233, U235, U238 and Pu239 measured by parallel plate ion chambers for the basic plutonium assembly 3B-2 given in Table 12, together with some calculated values. The values obtained by one-dimensional diffusion theory are always remarkably less than the measured fission rate ratios except the U233 to U235 fission ratio which is always overestimated in calculations. Calculations with the ABN set (not shown in the Table) gave somewhat better agreement between theory and experiment.

However, the deviations between calculated fission ratios in the range of 2-6 % are less than the discrepancy between calculated and measured values. The facts are not completely understood yet. Besides suspected cross section errors, it was found that actual reaction rates in cavities of a heterogeneous reactor do not compare with those from homogeneous calculations.

9.2 Reaction Rate Traverses

Radial and axial traverses for fission of U235, U238, Np237, Pu239 and capture of B10 were measured with small cylindrical chambers in assembly 3B-2 only. Fission rate traverses of U235 and U238 as well as capture rates of U238 were measured with foils also.

Within the core regions the measured traverses compare in shape quite well with the calculated ones. In crossing the core blanket boundary the deviations increase rapidly as shown in Fig. 15 for the ratio of calculated to measured (with chambers) Pu239, U235, and U238 fission rates in assembly 3B-2. The detailed behaviour of the discrepancies depends on the cross section set used in the caculations, but, as is known from earlier measurements /2/, the reaction rates in the blanket are mostly strongly underestimated by the calculations.

Within the inner core region axial and radial bucklings were derived from the measured traverses. They are given in Table 13 for chamber measurements and in Table 14 for foil measurements on the core axis for assembly 3B-2.

In measuring the foil traverses care was taken to always place the foils on corresponding locations in the unit cell, thus avoiding a distortion of the results by the flux fine structure. The experimental bucklings are smaller by up to 5 % than those derived from calculated reaction rate traverses.

Also fission rate ratios along the main axis of the reactor were obtained from the measured traverses by calibrating the cylindrical fission chambers against the parallel plate chamber at the core center. Except for the core blanket interface and blanket regions the traverses of the reaction rate ratios are almost constant over the main part of the assembly. The deviations from theory are the same als for spectral indices measured by the parallel plate ion chambers at the core center. However, it was found by one-dimensional calculations in plate geometry that the material surrounding the fission chambers due to its composition different from that of the core material shifted the neutron spectrum at the chamber positions to lower energies so that a somewhat softer spectrum than in the reactor was observed. Measured reaction rate ratios, therefore, can be used as spectral indices with precautions only in this case.

Apart from the experimental uncertainties it is believed that the deviations between calculated and measured spectral indices indicate some cross section errors in the group sets used and that in the calculations the neutron population in the blanket is underestimated due to inadequate theoretical treatment of self-shielding.

10. Central Reactivity Worth Measurements

10.1 Experimental Procedure

Central reactivity worths were measured in assemblies 3B-2 and 3B-2S. The samples were contained in 2.5 x 5.1 x 5.1 cm boxes which fit into a compartment of the horizontal drawer. The other compartments were filled with core material. The boxes were inserted and withdrawn by the automatic sample changer.

Most of the samples had a cross section of 4.6 x 4.6 cm, with thicknesses ranging from o.ol to 2.5 cm. Table 15 shows the composition of the fuel material samples. They were investigated in boxes with fuel and structural material. The reactivity effect was determined with the inverse kinetics programm KINEMAT /20/; corrections for first order reactivity drift, and for the transport of precursors by the drawer, were applied.

10.2 Calculational Methods

In most cases, the reactivity worths were calculated by two different methods. One is the first order perturbation theory, where a small amount of sample material is added to the core material. However, as this method is strictly correct only for very thin samples, a method was developed to account for the finite sample size /21/. It is based on the collision probability formalism for two zones, namely the sample and the surrounding core. It includes resonance effects, but does not take in account the heterogeneous structure of the surrounding core.

The unperturbed fluxes were obtained by one-dimensional diffusion theory in cylindrical geometry, using the KFK-SNEAK cross section set /7,8/.

10.3 Sample Size Effects

Samples of different thickness were measured in 3B-2 to study size effects. Some of the results are shown in Fig. 16 - 18, together with values calculated by the collision probability method. In general, the qualitative behaviour is predicted correctly, but the magnitude of the effect is underpredicted.

Sample size effects are most pronounced in strong absorbers, which are not present in the core like Ta and B10. For these materials, the agreement is satisfactory; however, the Ta samples were so thick that they are already in the flat portion of the curve.

CH_2 is an example for a pure scatterer, with a positive degradation effect, and a negative effect due to the reduction of self-shielding for the core materials upon insertion of the sample. The latter effect is strongly size-dependent, so that the worth increases with thickness. Calculation and experiment agree well.

The situation is more complicated for U238. Because it is present in the core, the neutrons impinging on the sample have already the resonance structure of U238, though for different dilution. The size dependence is predicted very poorly: The effect of the smallest and the largest sample differ by 16 %, but the calculation gives only 6 %. U235 shows a weak size effect, which is underpredicted.

10.4 Results

The results of experiment and calculation for 3B-2 and 3B-2S are given in Table 16. For 3B-2, the agreement between calculation and experiment is generally satisfactory. In particular, there is good agreement for U5, Pu9, Ta, CH_2, and Ni. The worths of the following materials are overpredicted by 10-15 %: U8, B10, Mo, Al, whereas SS is underpredicted by 8 %. In view of the existing uncertainties in β_{eff} and in the spectrum, one cannot conclude that the cross sections of these materials are in error, unless this conclusion is supported by other experiments. Strong discrepancies exist for Nb, where certainly the cross sections are in error, for C12, where, however, the experimental error was very large, and for Al_2O_3, where the sample was so large that the assumptions of the collision probability method are questionable.

In assembly 3B-2S, the agreement is generally much worse than in 3B-2, indicating that the characteristics of that assembly is not well understood.

11. Doppler Effect

Doppler reactivity measurements were carried out in the center of some of the 3B cores, using the technique of oscillating a hot versus a cold sample in the pile oscillator. The resulting changes in reactivity were obtained by solving the inverse kinetics equations. Samples of depleted uranium oxide and plutonium oxide were measured, they were heated up to 1000°K. The experimental equipment is described in detail in /22/. The data of the samples are given in Table 17.

In addition to the pile oscillator measurements, experiments on U238 with the SNEAK Doppler Loop were carried out. In the loop, a zone of 5 liters can be heated up to about 600°K.

11.1 Doppler Effect of U238 with the Pile Oscillator

A depleted uranium oxide sample was measured in the 4 assemblies 3A-2, 3B-2, 3B-2S and 3B-Void. The results together with calculated data, are shown in Fig. 19. The calculations were carried out by a method which includes resonance interaction between the sample and the environment, it is discussed in / 23 /. The spectra were taken from one-dimensional calculations with the original SNEAK-NORM set. They differ very little from heterogeneity corrected spectra. Expansion effects are small and were not corrected for. However, a correction for the influence of crystal binding in UO_2 was applied based on the concept of an effective temperature. The experimental phonon spectrum by Dolling / 26 / was used.

In 3B-2, the calculation underestimates the effect by about 6-7 %. The change to the harder spectrum of 3B-2S is overestimated; the effect in the much harder spectrum of the void core is also calculated within 10%. For comparison, the results for assembly 3A-2 are also shown. In this core, the good agreement is certainly fortuitous.

11.2 Doppler Effect of Pu239 with the Pile Oscillator

a.) Experiments to Determine Alpha of Pu239

Most of the Doppler effect of Pu239 in the spectra under investigation occurs between 200 eV and 5 keV. There has been much discussion recently on the α-value in this range and the Doppler measurements with Pu-samples were designed to give additional integral information on α.

The Doppler effect of Pu239 is composed of a positive fission contribution and a negative absorption contribution of similar megnitude, resulting in a rather small net effect which may be difficult to measure. Therefore, the measurements in 3B-2 were carried out in the normal core and, in addition, in a boron environment. In the eight elements surrounding the Doppler element, Pu239 was removed and replaced by such an amount of B_4C that the absorption at Doppler energies was kept the same. This replacement resulted in a considerably lower importance at Doppler energies, whereas the fluxes and the fission neutron importance were essentially kept the same (except for the different normalization). This way, the absorption contribution was considerably reduced, resulting in a fairly large positive Doppler effect of Pu239. The atom density of B10 was about 8×10^{20} at/cm^3, which is much lower than in earlier experiments at Argonne /27/.

Pu samples have a large reactivity effect of expansion /27/. However, the ratio of expansion to Doppler effect is much more favourable if the samples contain a diluent. In the samples used in SNEAK the PuO_2 was diluted with Al_2O_3. The rather small expansion effect was calculated as described in /23/.

Kelber and Kier /28/ found that the Doppler changes in the resonance integrals in the unresolved range of Pu239 in a mixture with U238 can only be calculated with a large variance due to the statistics of overlap with U238 resonances. However, it could be demonstrated by calculations that the variance is much smaller for a sample measurement, where the U238 resonances remain unaffected. The uncertainty in the calculated Doppler effect due to overlap statistics should be at most 20%.

The results for a PuO_2 sample are shown in Fig. 20. Calculations were carried out with two sets of resonance parameters, namely with those of Schmidt / 25 / ("Low α"), and with those obtained by Pitterle / 29 / from measurements of σ_t and σ_f ("High α"). Corrections for the radial expansion effect were applied. It is obvious from the figure that the experiments, both in the normal and in the boron environment, confirm the "High Alpha". The agreement is within 20 to 30 %, which is about the accuracy to be expected. Thus, the measurement with Pu samples can be interpreted conclusively.

b.) Experiments with PuO_2 Samples in a Boron Environment to Eliminate the Overlap Effect.

In order to investigate the influence of resonances of U238 on the Doppler effect of Pu239, which has been estimated to be small in a sample experiment, an experiment was carried out where this effect was not present. The PuO_2 samples were measured in an environment, consisting of 8 SNEAK elements, where U238 was removed, and replaced by an equivalent amount of B_4C. As the SNEAK plutonium is in the form of mixed oxide, it was necessary to remove also the Pu, and replace it by highly enriched uranium.

The results of the measurements in this environment are shown in Fig. 21 together with calculations using the "High Alpha" data. For the larger PuO_2 sample, the results are similar to those in the normal core. However, for the smaller sample, the scatter of the experimental points is large indicating a much larger statistical uncertainty than the evaluated one. Thus, this second measurement cannot be well interpreted. One can tentatively conclude from the experiment with the larger sample that the overlap effect is small, thus, confirming the statistical estimate. However, it must be emphasized that this conclusion is not very well founded.

c.) Experiment with a PuO_2 Sample in 3B-0.

The larger Pu sample was also investigated in the void-core 3B-0. In this hard spectrum, the calculated Doppler effect is positive, but small. The negative expansion effect is larger in magnitude than the Doppler effect so that the total calculated effect is negative. The agreement between experiment and calculation is slightly worse than in the 3B-2 experiments.(Fig.22)

However, because of the large expansion effect one can only conclude that the order of magnitude of the Doppler effect is calculated correctly.

11.3 Measurements with the Doppler Loop

A Doppler loop was installed in SNEAK, in which a central zone of 5 liters could be heated up to 600°K. The loop zone consisted of 9 subassemblies of 2o cm height. Each subassembly was filled with 49 pins of fuel and structural material with a diameter of 6 mm. It could be heated and cooled in cycles of several minutes by passing CO_2 through the zone. A large effort was made to minimize movement of the fuel by thermal expansion. The loop, which was similar to a Doppler loop used earlier in ZEBRA /3o/ was connected to a system of heaters, blowers, and ducts, which will probably be described in a later report by Däunert.

The Doppler loop was designed and built, in addition to the equipment for small-sample experiments, for the following reasons:

a) Typical core compositions should be built up in the loop, so that the Doppler effect of the actual case could be measured.

b) The loop zone was large enough to insure a significant reactivity change, and nearly large enough to establish its own neutron spectrum.

c) The loop was designed to largely avoid difficulties which were expected to be significant in the small-sample experiments, the interaction between resonances of the hot sample and the cold environment and the reactivity effect of thermal expansion.

In the experiment in assembly 3B-2, each of the 9 subassemblies of the Doppler loop was loaded with 29 pins of natural uranium and 2o pins of graphite. This composition was chosen such that the neutron spectrum in the loop at Doppler energies (o.1 - 2o keV) was about the same as in the surrounding core. Indeed, the fission rate of U5 and the capture rate in B10 are rather flat /Fig. 23/. However, the adjoint fluxes at low energies dipped by about 3o %; this is reflected in the distribution

of the reactivity worth of B10, which has about the same shape as the distribution of the Doppler effect. The average atom densities in the loop are given in Table 18.

The calculations were done by the usual methods, working with equivalent potential cross sections which were determined in a way similar to the one used by Rowlands and Wardleworth /31/. The resonance paramenters were the same as used for the interpretation of the pile oscillator measurements.

The experimental and calculated reactivity changes are shown in Fig. 24. The calculation underestimates the effect by about 10 %. This result is well in line with the results of the pile oscillator measurements, where the difference was about 6-7 %. Thus, the two different experimental techniques and their interpretation lead to the same results.

12. Prompt Neutron Decay Constants

Prompt neutron decay constants were measured in the standard core 3B-2 only. For these measurements the pulsed neutron technique and the Rossi-α method were applied. Due to some systematic errors in the pulsed source measurements partly caused by the influence of higher harmonics in the prompt decay of the neutron pulse only the results of the Rossi-α experiments could be evaluated.

In contradiction to earlier statements / 32 / it was demonstrated for the first time that Rossi-α measurements can be performed in fast reactors containing more than 100 kg of plutonium and that good results can be obtained from signals having signal-to-background ratios of a few percent when adequate techniques are applied. In detailed theoretical and experimental investigations / 33, 34 / it was shown that conventional techniques used so far are upset by systematic errors due to deadtime effects in the time analyzer. These difficulties were overcome by decreasing the deadtime in the pulse channels as well as in the trigger channel of the time analyzer.

For the Rossi-α measurements on SNEAK-3B-2 3 fast He^3 proportional counters (thermal sensitivity 24 cts/n/cm^2 each) at position 20/19 in the center of the plutonium zone were used as neutron detectors. Their output pulses were amplified and shaped separately, then added to form the single detector signal to be analyzed. Time analysis was accomplished by using a fast

shift register controlling a number of 32 coincidence channels / 34 /. In this newly developed time analyzer the deadtime between successive cycles is only one channel width. Remaining deadtime effects were further reduced by chopping the trigger pulses.

The Rossi-α was measured for several subcritical states ranging from -1.5$ to -5$. Only one exponential without any contribution of other modes from the outer driver zones was found by fitting the experimental data.

In Fig. 25 the measured values of α were plotted against the mean time distance 1/b between two detector pulses (b=counting rate, ranging from 30000 to 130000 cts/sec), which is a measure of reactivity. The prompt neutron decay constant of the critical reactor is obtained by extrapolation to 1/b=0:

$$\alpha_c = 1.25 \times 10^4 \ (\text{sec}^{-1}) \pm 4\%.$$

Scaling of the abszissa 1/b in $'s can be achieved by further extrapolation to prompt critical, i.e. α=o yielding the abszissa corresponding to $\rho^+ = +1\$$. For the same reason the value $\alpha = 2\alpha_c$ corresponds to $\rho^+ = -1\$$. Subcriticalities evaluated in that way /Fig. 25/ agreed very well with reactivities determined with inversed kinetics programs.

13. Calculated Kinetics Parameters

One dimensional diffusion calculation in cylinder geometry with the original SNEAK set yielded the following kinetics parameter for assembly 3B-2

neutron life time l	=	$4.285 \cdot 10^{-7}$ sec
delayed neutron fraction β_{eff}	=	$4.617 \cdot 10^{-3}$
prompt neutron decay constant $\alpha_c = \frac{\beta_{eff}}{l}$	=	$10.78 \cdot 10^{3}$ sec^{-1}

The β_{eff} of $4.976 \cdot 10^{-3}$ which was used for the evaluation of all reactivity measurements had been calculated with preliminary core dimensions in cylindrical geometry. It would therefore appear that the correct value is closer to the new results of $4.617 \cdot 10^{-3}$, although inclusion of the axial

blanket contribution would again raise the value and partially compensate for the difference.

The calculated α_c values for assembly 3B-2 are by 14 % less than the experimental value in contradiction to the well-known overestimation of the prompt neutron decay constant for other fast reactors. In assembly 3A-2, for instance, which is similar to assembly 3B-2 except for the central plutonium zone α_c is overestimated by the same calculational techniques by 23 %. Since the prompt neutron decay constant can be interpreted as a spectral index which depends strongly on the low energy part of the spectrum one might conclude that this discrepancy is due to incorrect treatment of the low energy spectrum and inadequate neutron lifetime calculations. One also has to account for the errors due to the inadequate one-dimensional calculations of β_{eff} and due to the fact that the calculated reactors were subcritical and not identical with the actual assemblies, because for the measurements in one subassembly at the core center the fuel was almost completely replaced by the He^3-detectors. The resulting reactivity effect was compensated by exchange of blanket elements by core elements. The different influence of all of these error sources on the prompt neutron decay constants of the assemblies 3A-2 and 3B-2, however, is not understood yet and will be further investigated.

In this context, it is interesting to compare the measured and calculated central reactivity worth of core material in 3A-2 and 3B-2. This worth, per unit volume, is simply given by the expression

$$\rho = \frac{\bar{\bar{D}}\, B_m^2}{\beta_{eff}\, F} ,$$

where $\bar{\bar{D}}$ is the flux and adjoint weighted diffusion coefficient, B_m^2 is the material buckling of the central zone, and F is the normalization integral.

The results are for 1 cm^3 of core material

	3A-2	3B-2
Experiment, m$	0.269	0.380
Calc./Exp., SNEAK (final)	0.94	1.07
Calc./Exp., ABN	0.94	1.08

The important point about this result is that the ratio Calc./Exp. differs by 14% between the two assemblies, although the differences in B_m^2 and in the diffusion coefficient are small, and fairly well known from the substitution experiment. This seems to indicate that the delayed neutron data of the two assemblies are not consistent. However, one has to be cautious because the experimental results are uncertain due to environmental effects, which are not fully understood. To sum it up, a smaller β_{eff} for 3A-2 and a larger one for 3B-2 would give better agreement with calculation for both the Rossi-α experiment and the reactivity worth of core material.

References

/ 1/ Stegeman, D. et al.: "Physics Investigations of a 670 l Steam Cooled Fast Reactor System in SNEAK, Assembly 3A-1"
KFK-627 (1967)

/ 2/ Schröder, R. et al.: "Physics Investigations of Uranium-Fueled Fast Steam-Cooled Reactors in SNEAK, Assemblies 3A-0, 3A-2, 3A-3"
KFK-847 (1968)

/ 3/ Schröder, R.: "Zur Simulation von Spaltprodukten in schnellen kritischen Anordnungen "
Nucleonik 10, 18, (1967)

/ 4/ M. Barberger et al.: "Progressive Substitution Method in Fast Multinzone Experiments"
ANL-7320, (1966) pg. 429

/ 5/ F. Storrer and J.M. Chaumont: " The Application of Space-Energy Synthesis to the Interpretation of Fast Multizone Critical Experiments"
ANL-7320 (1966) pg. 439

/ 6/ F. Helm: "A Method of Evaluating Progressive Substitution Experiments for the Determination of Bucklings and Critical Radii"
KFK-975, EUR 4175e (1969)

/ 7/ Bachmann H., Huschke H. et al.:"The Group Cross Section Set KFK-SNEAK Preparation and Results"
KFK-628 (1967)

/ 8/ Huschke H.: "Gruppenkonstanten für dampf- und natriumgekühlte schnelle Reaktoren in einer 26-Gruppen Darstellung"
KFK-770 (1968)

/ 9/ Pönitz, W.P. et al.: "Some New Measurements and Renormalizations of Neutron Capture Cross Section Data in the keV Energy Range"
KFK-635 (1967)

/10/ Schomberg, M.G. et al.: "A New Method of Measuring Alpha (E) for Pu239" , Proceedings of the IAEA Symposium, Karlsruhe (Oct. 67)

/11/ E. Kiefhaber et al.: "Evaluation of Fast Critical Experiments by Use of Recent Methods and Data" , BNES Conference on : The Physics of fast reactor operation and design, pg. 94, London, 1969

/12/ Abagjan, L.P. et al.: German Translation of "Group Constants of Fast and Intermediate Neutrons for the Calculation of Nuclear Reactors" States Comittee for the Use of Atomic Energy in the USSR

/13/ Wintzer, D.: "Zur Berechnung von Heterogenitätseffecten in periodischen Zellstrukturen thermischer und schneller Kernreaktoren" KFK-743 (1969)

/14/ Bluhm H., Stegemann D.,: "Theoretical and Experimental Investigation for an Improved Application of the Li^6-Semiconductor Sandwich Spectrometer" Nucl. Instr. Meth. 7o (1969) 141

/15/ Pendlebury E.D. "Neutron Cross Sections of Li^6 in the Energy-Range 0.001 eV - 15 MeV. AWRE-Report No. O-60/64 (1964)

/16/ Yates, N.I.L., Private Communications

/17/ Bennett, E.F.: "Fast Neutron spectroscopy by proton recoil proportional counting" Nucl. Sci. Eng. 27 (1967) 16

/18/ Benjamin P.W., Kemshall C.D., Redfearn J.: "The Use of a Gas-Filled Spherical Proportional Counter for Neutron Spectrum Measurements in a Zero Energy Fast Reactor , AWRE-Report No. NR 2/64 (1964)

/19/ Bluhm H., Fieg G., Kappler F., Kuechle M., Müller M., Werle H., Wattecamps, E.: Neutron Spectrum Measurements in Various SUAK Assemblies. BNES Conf. Fast Reactors, London (1969)

/20/ W.J. Oosterkamp, KFK-1036 (1969)

/21/ E.A. Fischer, KFK-995 (1969)

/22/ L. Barleon, to be published

/23/ E.A. Fischer, KFK-844 (1969)

/24/ J.B. Garg et al., Phys. Rev. 134, B985 (1967)

/25/ J.J. Schmidt, KFK-120 (1966)

/26/ G. Dolling et al., Can. Journ. of Phys. 43, 1397 (1965)

/27/ G.J. Fischer et al., Nucl. Sci. and Eng. 25, 37 (1966)

/28/ C.N. Kelber and P.H. Kier, Nucl. Sci. and Eng. 24, 389, and 26, 67 (1966)

/29/ T.A. Pitterle, E.M. Page, and M. Yamamoto: "Calculations of Fast Critical Experiments Using ENDF/B Data and a Modified ENDF/B Data File", Second Conference on Neutron Cross Section Technology, Washington, March 1968

/30/ A.R. Baker and R.C. Wheeler, ANL-7120, p. 553 (1965)

/31/ J.L. Rowlands and D. Wardleworth, ANL-7120, p. 566 (1965)

/32/ R.S. Brunson, R.N. Curran, J.A. Gasidlo, and R.J. Huber: " A Survey of Prompt Neutron Lifetimes in Fast Critical Systems", ANL-6681 (1963)

/33/ H. Borgwaldt: "Einheitliche Theorie der Korrelationsexperimente in Nulleistungsreaktoren" Externer Bericht, INR-4/66-5 (1966)

/34/ M. Edelmann: "Neue Methoden zur Rossi-α Messung" Externer Bericht INR-4/68-15 (1968)

Table 1

Contents of Fission Products Mock-up Platelets

Material	Amount per 100 platelets (g) (Mixture I)	Amount per 100 platelets (g) (Mixture II)
MoO_3	366,4	366,4
Ag_2O	80,0	41,1
Cd	5,0	5,0
AgI	16,1	16,1
$CsNO_3$	44,6	44,6
La_2O_3	63,4	63,4
CeO_2	137,2	137,2
Pr_6O_{11}	55,9	57,7
Nd_2O_3	330,7	208,8
Sm_2O_3	89,1	89,6
Eu_2O_3	7,9	7,9
Gd_2O_3	3,7	3,7
Ru		134,4
Rh		39,0
Pd		109,8
	1200,0	1324,7

Table 2

Atom Densities (in 10^{20} cm^{-3}) of SNEAK Assembly 3B Used for Homogeneous Calculations[a]

3B-2

	Pu zone	U zone 1	U zone 2	Inconel	Zone with fission products	Blanket
Pu239	14,76			14.76	14.76	
Pu240	1.33			1.33	1.33	
Pu241	0.11			0.11	0.11	
Pu242	0.06			0.06	0.06	
U235	0.56	20.404	20.25	0.56	0.56	1.625
U238	81.86	81.39	81.26	81.86	81.86	399.414
Al	125,6	129.66	129.47	127.4	126.4	
C	9,73	8.76	9.00	9.56	9.73	0.14
Co	0.14	0.18	0.19		0.14	
Cr	33,72	34.09	34.31	17.41	33.72	11.08
Fe	119.7	120.47	121,16	61.99	119.7	39.55
H	18.49	16.81	17.29	18.49	18.49	
Mg	1.31	0.65	o.65	1.33	1.31	
Mn	2.23	1.99	1.97	1.47	2.23	0.87
Ni	17.55	18.43	18.23	95.00	17.55	9.84
O	122.2	146.28	145.8o	122.2	128.2	
Si	2.54	1.84	1.86	1.79	2.54	0.46
Ti	0.30	0.38	0.39		0.30	
Mo	0.29	o.40[b]	0.40[b]	8.85	0.29	0.19[b]
Nb	0.09			0.05		
SPP (fission products).					2.72	

[a] for the calculations Co was added to Fe, Mg to Al, Mn to Cr, and Nb to Mo.

[b] includes Nb-concentration

Table 3

Results of SNEAK Substitution Experiments

Experiment	Step	Result of Fit after this Step							
				ΔD/D free parameter			ΔD/D fixed parameter[+)]		
		r_z	Δr_c	$\frac{\Delta B_r}{B_r}$	$\frac{\Delta D}{D}$	$\Delta_o r_c$	$\frac{\Delta B_r}{B_r}$	$\Delta_o r_c$	
SNEAK-3A2 → SNEAK-3B2 Uranium → Plutonium	1	3.07	-0.017						
	2	6.86	-0.068						
	3	9.21	-0.138				0.0111	-1.26	
	4	14.06	-0.188	-0.6877	1.515	20.0	-0.0210	0.53	
	5	18.67	-0.26	0.0233	-0.0454	-0.79	-0.0174	0.34	
	6	23.17	-0.315	0.0194	-0.0365	-0.70	-0.0151	0.21	
	7	25.49	-0.366	0.0327	-0.0687	-1.01	-0.0129	0.08	
	8	25.86	-0.366	0.0314	-0.0655	-0.98	-0.0124	0.05	
	9	29.60	-0.326	-0.0097	0.0397	0.01	-0.0131	0.09	
	10	29.91	-0.322	-0.0133	0.0488	0.10	-0.0133	0.095	
SNEAK-3B2 → SNEAK-3B-Inconel	1	3.07	0.031						
	2	6.86	0.152						
	3	9.21	0.260	0.3873	-0.9176	-10.5	-0.0055	1.26	
	4	15.35	0.680	-0.1950	0.3332	7.0	-0.0173	1.87	
	5	20.59	1.099	-0.0093	-0.0905	1.63	-0.0166	1.84	

[+)] = 0.0502 (U Pu)

= 0.0733 (Inconel)

r_z = Radius of substituted zone

Δr_c = change in critical radius

$\Delta_o r_c$ = change in critical radius extrapolated for substitution throughout the core

Table 4

Results of Complementary Substitution Experiments

Material in substituted zone	Surrounding material	Zone dimensions	$\Delta k (10^{-4})$
3B-2-composition	3A-2-composition	central element	1.251
"	"	2 elements at r=21.76 cm	3.o8
3A-2-composition	3B-2-composition	central element	1.06
"	"	2 elements at r=16.32 cm	1.23
"	"	9 central elements axial zone 1[a)]	0.14
"	"	9 central elements axial zone 2	0.51
Inconel composition	3B-2-composition	1 central element	-1.91
"	"	9 central elements axial zone	-3.87
"	"	9 central elements axial zone 2	-5.18
3B-2-composition	Inconel-comp.	9 central elements axial zone 1	4.14
3B-2-composition	"	9 central elements axial zone 2	4.67

a) Axial zone 1 extends from -5.024 to +5.024 cm, measured from the midplane

b) Axial zone 2 extends from -25.12 to -15.o72 plus from +15.o72 to +25.12 cm measured from the midplane.

Table 5

k_{eff} Calculated for Critical Configurations

Cross section set / Assembly	SNEAK (original)	SNEAK (final)	PMB	PMB-α	MOXTOT[b]	ABN	Heterogeneity correction
3A-1	0.9895				1.014	1.019	
3A-2	0.9835		0.9795		1.005	1.006	4.31×10^{-3}
3B-2	0.9750	0.9791	0.9793	0.9652	0.993	1.0216	2.55×10^{-3}
3B-2 Inconel	0.9731	0.9769	0.9771	0.9636		1.0180	3.89×10^{-3}
3B-2S	0.9647	0.9686	0.9687	0.9556		1.0119	
3B-2 extrapolated (R_o=44.97 cm)[a]	0.9678	0.9740	0.9767	0.9567		1.0265	2.06×10^{-3}
3B-2 Inconel extrapolated (R_o=46.9 cm)[a]	0.9625	0.968	0.971	0.951		1.018	

[a]The R_o are from a preliminary evaluation of the substitution experiment

[b]Two dimensional calculations

Table 6

Dimensions of Testzones for Void and Flooding Experiments

Zone No.	Description	Boundaries (cm, from core center). axial	radial
I	10 cm above and below midplane in 9 central elements	-10.075, + 10.075	9.21
II	9 central elements, total core height	-40.3 , + 40.3	9.21
III	21 central elements, total core height	-40.3 , + 40.3	14.06

Table 7

Void Experiments, $-\Delta k/k$ (%)

Assembly	Zone	Measured	Calculation		$\frac{\Delta k_{calc}}{\Delta k_{meas}}$	
			NORM	HET	NORM	HET
3A-1	III	o.459	o.382	o.4o6	o.84	o.83[a]
	total core	3.18 (extrap.)	2.64	2.79	o.84	o.83
3A-2	I	o.177		o.147		o.83
	II	o.498		o.413		o.83[b]
3B-2	I	o.o91	o.o87	o.1o4	o.96	1.14
	II	o.242	o.192	o.223	o.8o	o.92
	III	o.583	o.4oo	o.496	o.69	o.85
3B-2 Inconel	I	o.o88	o.o45	o.o67	o.51	o.76
	II	o.2o4	o.1o3	o.157	o.5o	o.77
3B-2S[c]	I	o.o6o	o.o48	o.o65	o.8o	1.o8
	II	o.171	o.o88	o.132	o.51	o.77
	III	o.386	o.187	o.287	o.48	o.74

[a] by k_{eff} Diff. calculations in plate geometry

[b] by perturbation calc. in plate geometry

[c] The calculated values are corrected for gaseous fission products considered in the data set but not present in the mock up plates and for inapplicable data for Sm and Gd which were originally prepared for thermal reactors.

Table 8

Flooding Experiments, $\Delta k/k$ (%)

Assembly	Zone	Measured	Calculation		$\frac{\Delta k_{calc}}{\Delta k_{meas}}$	
			NORM	HET	NORM	HET
3A-2	I	o.188	o.14o	o.153	o.74	o.81[a]
	II	o.517	o.373	o.4o8	o.72	o.79
	III	1.18		o.92		o.78
3B-2	I	o.122	o.o88	o.1o9	o.72	o.89
	II	o.344	o.231	o.276	o.67	o.8o
	III	o.782	o.5o7	o.6o5	o.65	o.77
3B-2 Inconel	I	o.1o1	o.o45		o.45	
	II	o.289	o.142		o.49	
3B-2S[b]	II	o.24	o.1o9		o.45	
	III	o.53	o.234		o.44	

[a] This perturbation results for Zone I was multiplied by a correction factor which for Zone II brings axial perturbation calculation and radial diffusion calculation into agreement.

[b] Calculated data corrected for gaseous fission products and for unapplicable Sm and Cd cross section in data set.

Table 9

A Comparison of the Effects of the Inconel and the Fission Product Modification

	Inconel		Fission Products	
	cale	measured	cale	measured
Δk_{eff} (%) upon introduction of modified zone	-o.77	-o.72	-1.42	-o.64
CH_2 [a] void effect:				
Zone I	-0.104 -0.067 +0.037	-0.091 -0.088 +0.003	-0.104 -0.065 +0.039	-0.091 -0.060 +0.031
Zone II	-0.223 -0.157 +0.066	-0.242 -0.204 +0.038	-0.223 -0.123 +0.091	-0.242 -0.171 +0.071
Zone III			-0.496 -0.287 +0.209	-0.583 -0.386 +0.196

[a] The data for Void effect are arranged as follows

Effect in the basic core
Effect in the modified core
Difference of the Effects

Table 10

Characteristics of materials used for foil activation

Isotop	Energy of main resonance (eV)	Form of material	Foil thickness (μ)	Number of resolved resonances
Na-23	2850	NaF	500	20
Cu-63	577	metal	100	31
Mo-98	467	metal	200	8
Mn-55	337	metal+ 12% Ni	50	35
Cd-114	120	metal	500	6
Br-81	101	UBr	500	3
La-139	72.4	metal	250	31
W- 186	18.8	metal	25	27
Sm-152	8.04	metal	75	1
Au-197	4.91	metal	25	5o
In-115	1.456	metal+ 50% Pb	50	11

Table 11

R and P_M for the investigated SNEAK assemblies

Material	3B-2 Normal		3B-2 Void		3B-2 Flooded		3B-2 Fission Product	
	R(%)	P_M(%)	R(%)	P_M(%)	R(%)	P_M(%)	R(%)	P_M(%)
Na-23	2.8	93.8	3.2	72.3	2.3	98.2	2.3	93.2
Cu-63	6.1	84.8	3.3	47.1	7.6	87.9	3.4	83.0
Mo-98	3.7	57.8	1.8	21.7	4.3	72.1	2.3	56.6
Mn-55	5.o	74.o	2.6	56.5	5.3	77.7	3.2	71.3
Cd-114	1.7	35.2	0.7	7.1	2.9	37.o	1.3	32.7
Br-81	9.6	32.3	3.0	5.1	13.2	35.6	6.0	30.5
La-139	7.6	9o.1	2.4	15.4	10.8	96.2	4.7	85.9
W-186	16.3	91.5	3.1	21.3	21.4	95.3	10.1	90.6
Sm-152	16.6	82.1	4.4		26.0	86.4	7.7	78.4
Au-197	9.9	72.2	1.7	8.7	17.6	9.5	5.9	71.1
In-115	14.o	96.9	2.2	-	21.6	98.1	8.8	93.8

Table 12

Measured and Calculated Fission Rate Ratios (to U235) at the Center of SNEAK-3B-2

	Experiment	Calculation (SNEAK-set, final version)
Th232	0.00640 ± 6%	0.004622
U233	1.47 ± 3%	1.506
U238	0.0289 ± 3%	0.02333
Pu239	0.938 ± 3%	0.8322

Table 13

Experimental Axial and Radial Bucklings from Chamber Traverses of Assembly 3B-2

	Position	Dist. from center axis (cm)	$10^4 \times B^2$ (cm^{-2})				
			U235	U238	Pu239	Np237	B10
Axial	2o/19	0	7.98	8.52	8.o4	8.44	-
	19/12	38.08	7.73	8.15	7.75	-	-
	2o/9	54.4	8.17	8.75	8.27	-	-
Radial	Midplane	-	8.7o	7.9o	8.17	8.26	9.16

Table 14

Axial Bucklings of Assembly 3B-2 (Foil Activations and Calculation)

Reaction	Buckling (10^{-4} cm^{-2}) Experiment	Calculation
U238-fis.	8.35	-
U238-capt.	8.7o	-
U235-fis.	-	8.56

Table 15

Composition of Uranium and Plutonium Samples

Sample		Weight refers to	Fuel composition (%)				Component other than fuel	Weight ratio: other component / fuel
Material	Weight (g)		U235	U238	Pu239 + Pu241[+)]	Pu240		
U235	all weights	U235 content	93.4	6.6	-	-	no	-
U238	all weights	total uranium	0.4	99.6	-	-	no	-
Pu	2.5	total plutonium	-	-	91.6	8.4	Al	78
	5.0	total plutonium	-	-	91.6	8.4	Al	63

[+)] $\frac{\text{Amount Pu241}}{\text{Amount Pu239}} < 1\ \%$

Table 16

Central Reactivity Worths, $10^6 \Delta k/k/g$

(Assuming $\beta_{eff} = 0.004976$)

	Sample Weight, g	Assembly 3B-2			Assembly 3B-2S		
		Experiment	Calc.Pert. / Exp.	Calc.Coll. / Exp.	Experiment	Calc.Pert. / Exp.	Calc.Coll. / Exp.
U235	3.4	3.77 ± 0.17	1.055	1.04	3.56 ± 0.05	1.17	1.15
	6.8	3.73 ± 0.05	1.065	1.05			
	15.0	3.63 ± 0.03	1.09	1.065			
U238	62.4	-0.275 ± 0.010	1.08	1.05	-0.246 ± 0.002	1.22	1.22
	124.3	-0.248 ± 0.005	1.20	1.14			
	249.1	-0.238 ± 0.005	1.25	1.18			
Pu	1.48	4.17 ± 0.20	1.06	1.06	3.97 ± 0.1	1.13	1.16
	2.50	4.39 ± 0.15	1.01	1.01			
	4.87	4.41 ± 0.10	1.00	1.01			
B-10	0.085	-145 ± 5	1.09	1.05	-137 ± 2	1.08	1.06
	0.307	-130 ± 3	1.22	1.10	-121 ± 1	1.22	1.14
	0.896	-111 ± 0.5	1.43	1.14	-106.5 ± 0.2	1.38	1.05
	2.50	- 97.5± 0.2	1.63	1.08			
Ta	53.7	-1.74 ± 0.02	2.67	1.05			
	107	-1.62 ± 0.02	2.87	1.01			
	160	-1.45 ± 0.02	3.20	1.01			
Mo	11	-0.58	1.68	1.33			
	34	-0.61	1.60	1.11			
	68	-0.55	1.77	1.13			
	102	-0.52	1.88	1.15			
Nb	28	-0.76		1.62			
	56	-0.72		1.55			
Ni	114	-2.13		0.96			
SS	109	-1.65		0.92	-1.50 ± 0.01	0.80	0.66
CH_2	1.1	9.3	1.01	1.07	6.6 ± 0.2	1.00	1.10
	2.1	10.5	0.90	0.98			
	4.6	11.2	0.84	0.99			
C	24	+0.081 ± 0.008		0.87			
	49	+0.020 ± 0.004		3.0			
Al	37	-0.154	1.12	1.08			
	147	-0.168	1.16	1.07	-0.140 ± 0.002	1.35	1.27
Al_2O_3	210	-0.109		1.25	-0.122 ± 0.001	1.82	1.52

Table 17

Data of Doppler Samples

Material	Enrichment	Length (cm)	Diameter (cm)	Weight (g)	
				U	UO_2
UO_2	0.4	9.0	3.5	773,9	877,9
	^{240}Pu content (%)			Weight (g) PuO_2	Al_2O_3
PuO_2	7.0	15.0	3.5	154.5	481.3
PuO_2	7.0	15.0	3.5	451.7	365.0

Table 18

Average Atom Densities in the Doppler Loop, 10^{20} At/cm^3

C	138
Cr	36.8
Fe	148
Ni	9.8
O	104.6
U5	0.37
U8	51.9

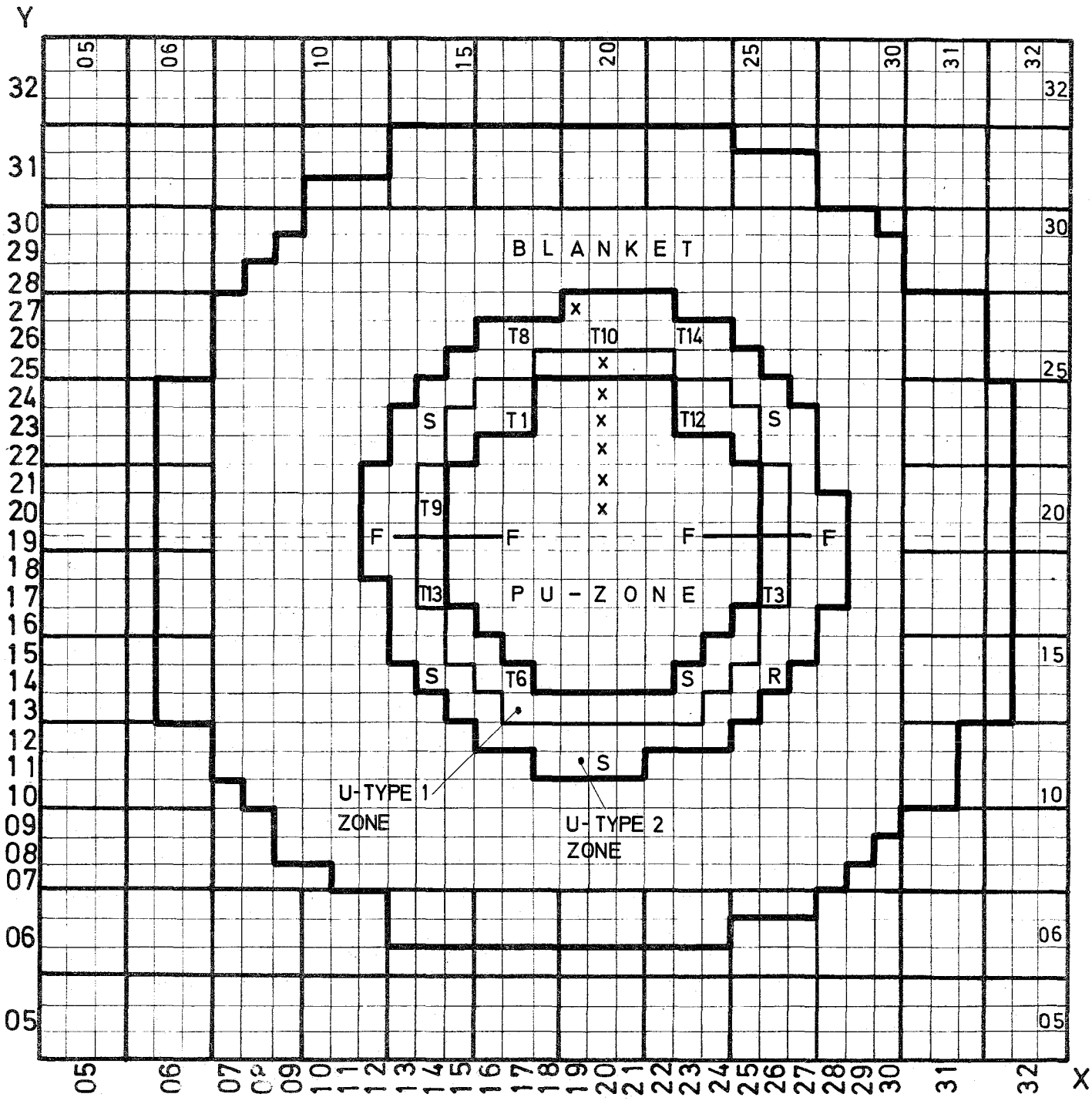

SNEAK- 3B 2

T Shim rods
S Safety rods
R Control rod
x Position with thermocouples
F–F Core elements with radial canal

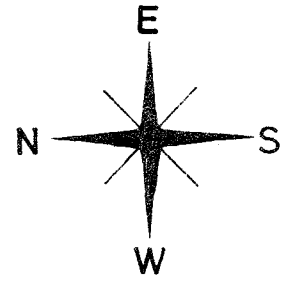

Fig. 1 Cross Section of SNEAK 3B 2

Scale 1:10

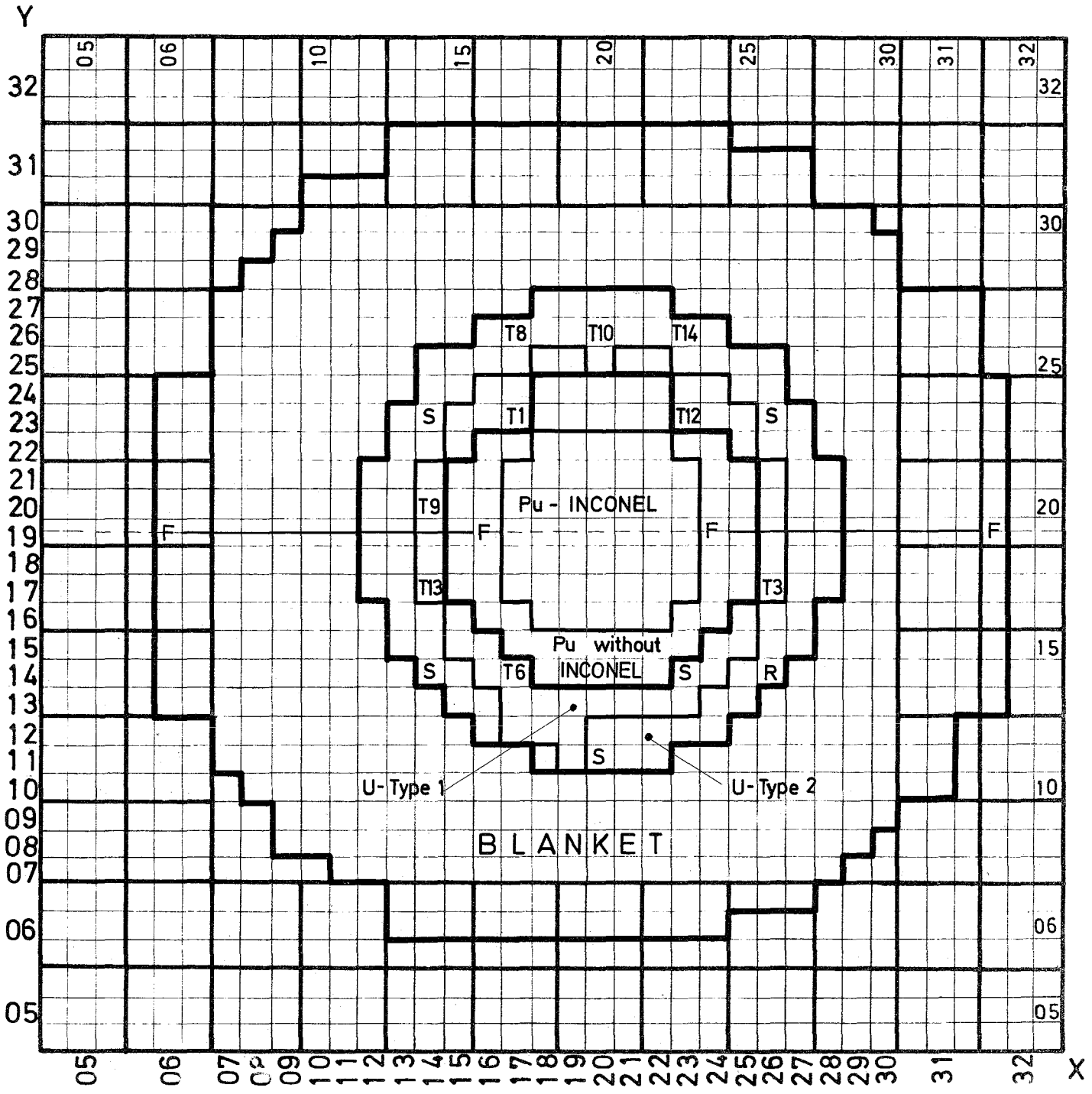

SNEAK- 3 B - 2 INCONEL

T Shim rod
S Safety rod
R Control rod
F - F Core element with window

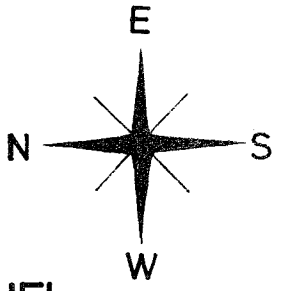

Fig.2 Cross Section of SNEAK 3B-2 INCONEL

Scale 1: 10

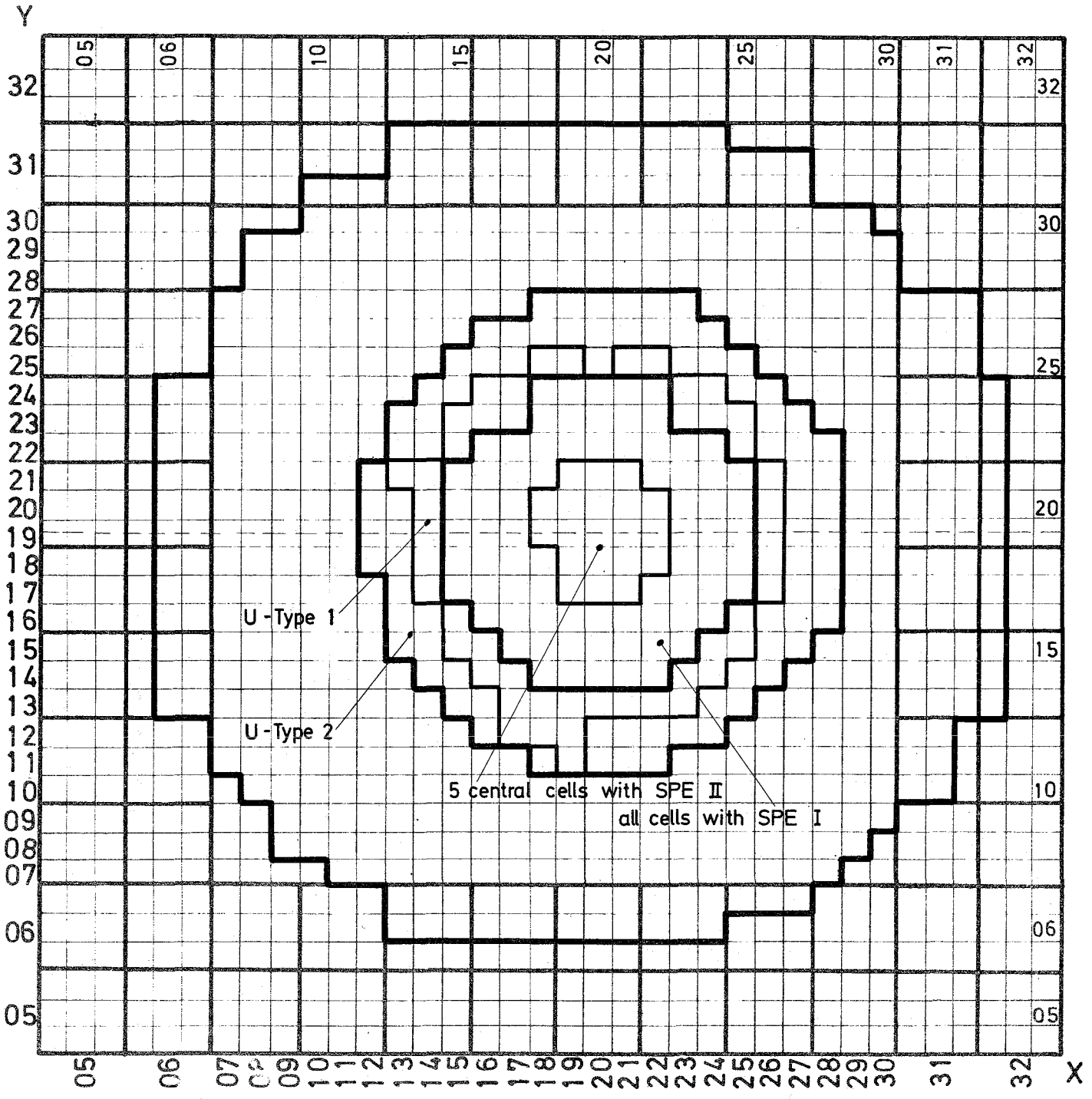

SNEAK- 3B2 -S

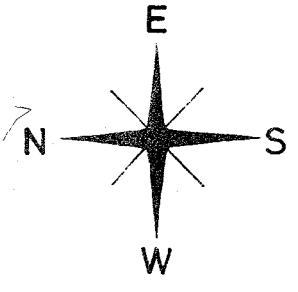

Fig.3 Cross Section of the Assembly
SNEAK - 3B2 - S

Scale 1: 10

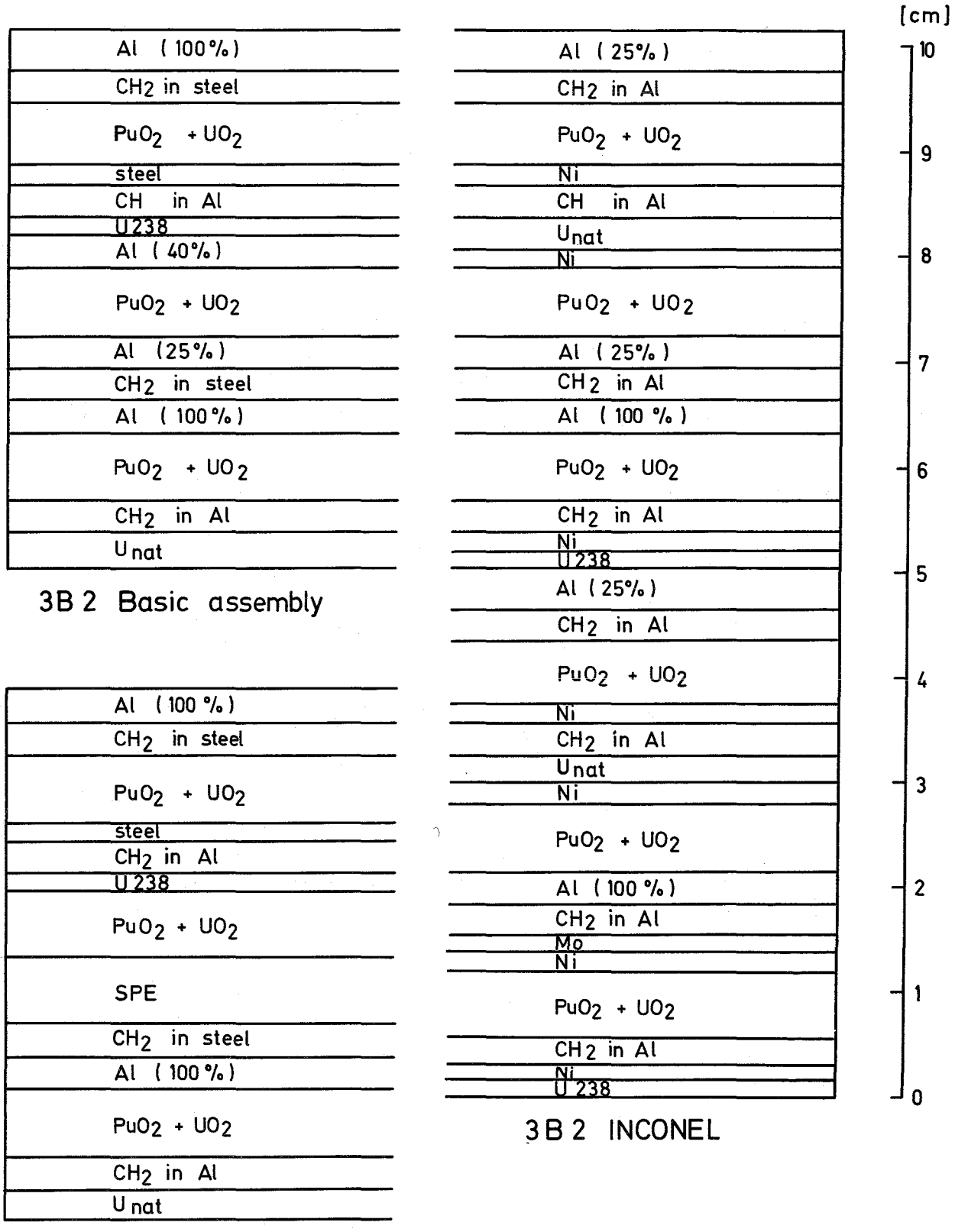

Fig. 4 Unit Cells for Plutonium Zones of SNEAK 3B

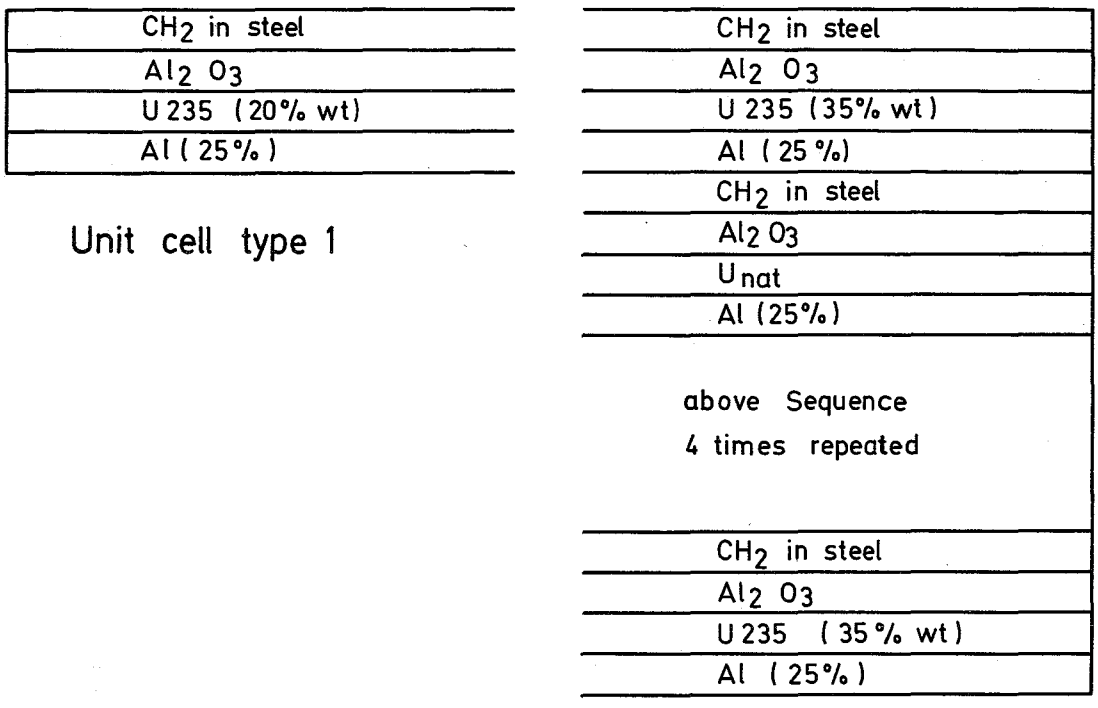

Fig. 5 Unit Cells for Uranium Zones in SNEAK 3B

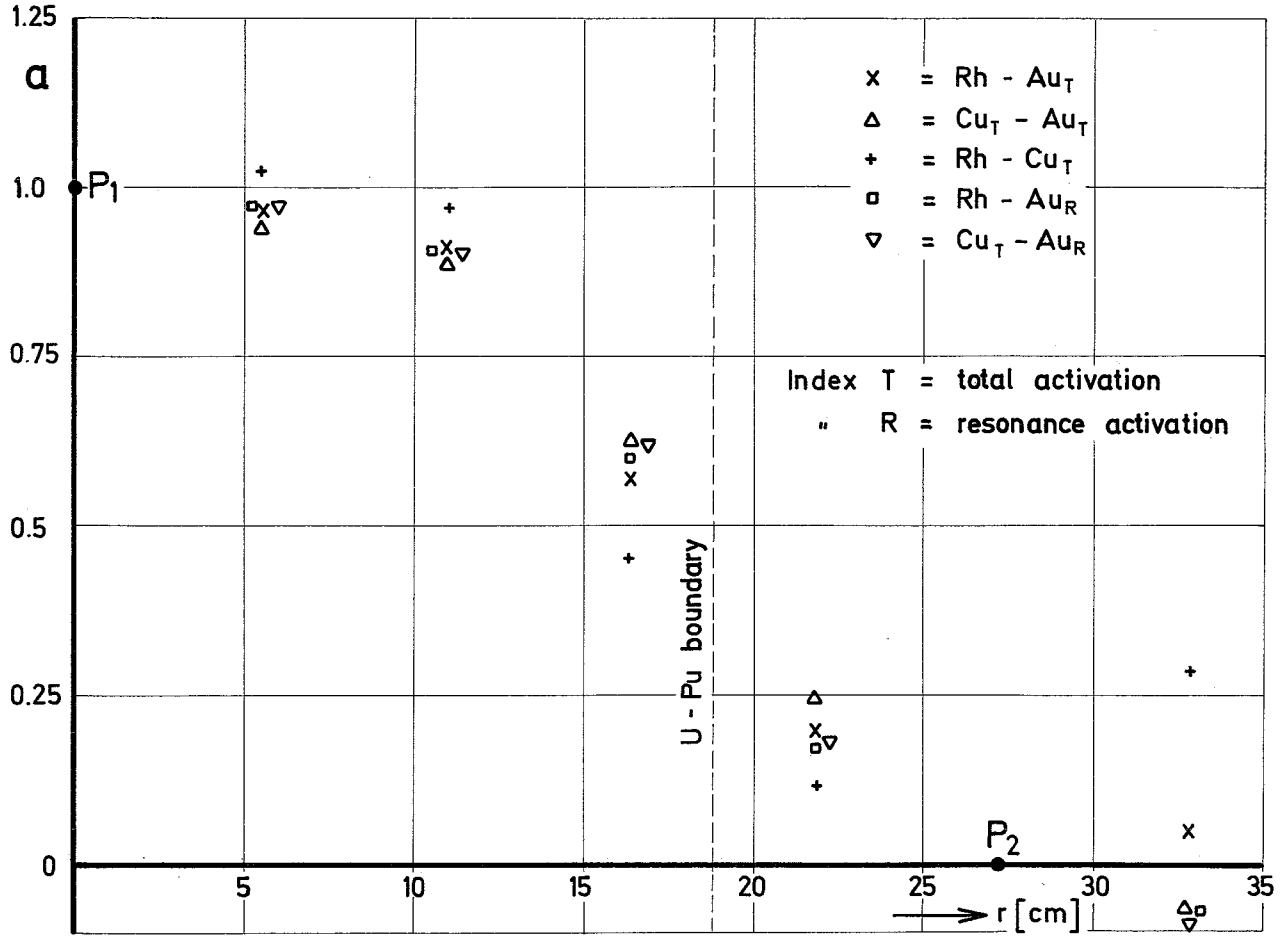

Fig. 6 Coefficients for Flux Synthesis

Radius of Pu - Zone = 18.7 cm

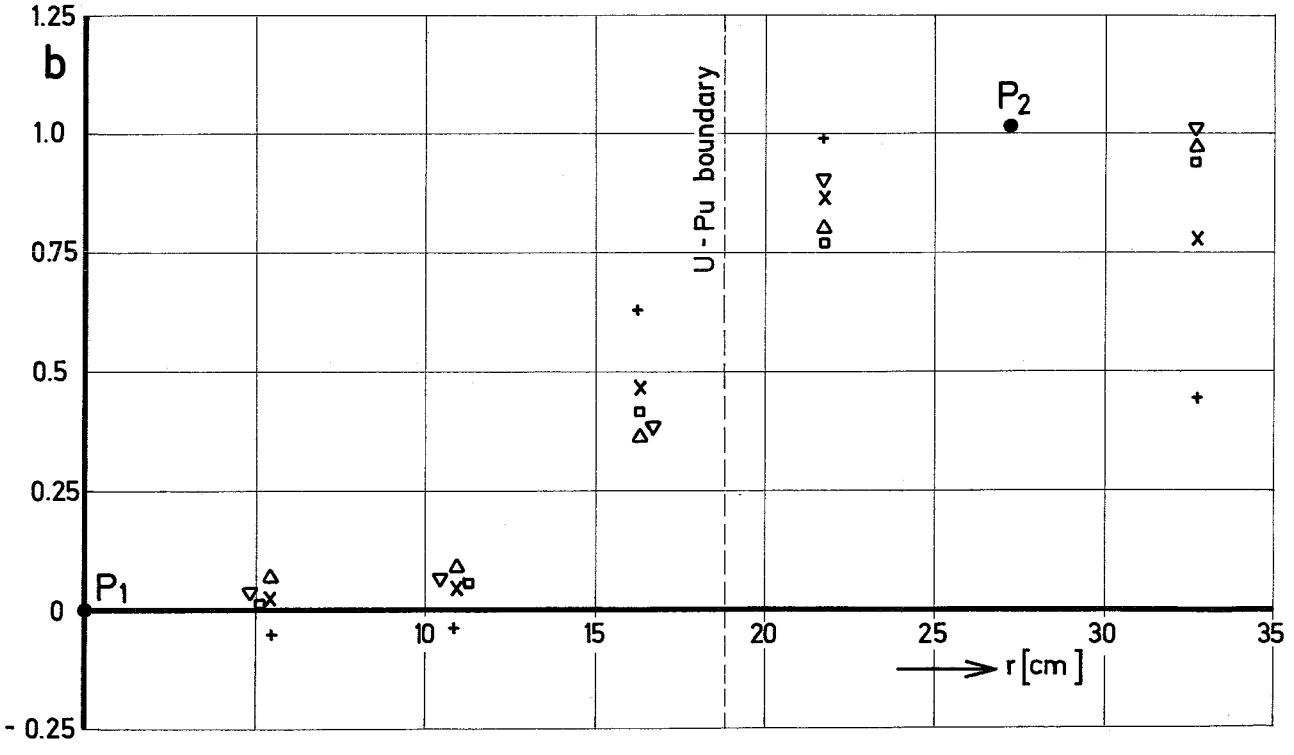

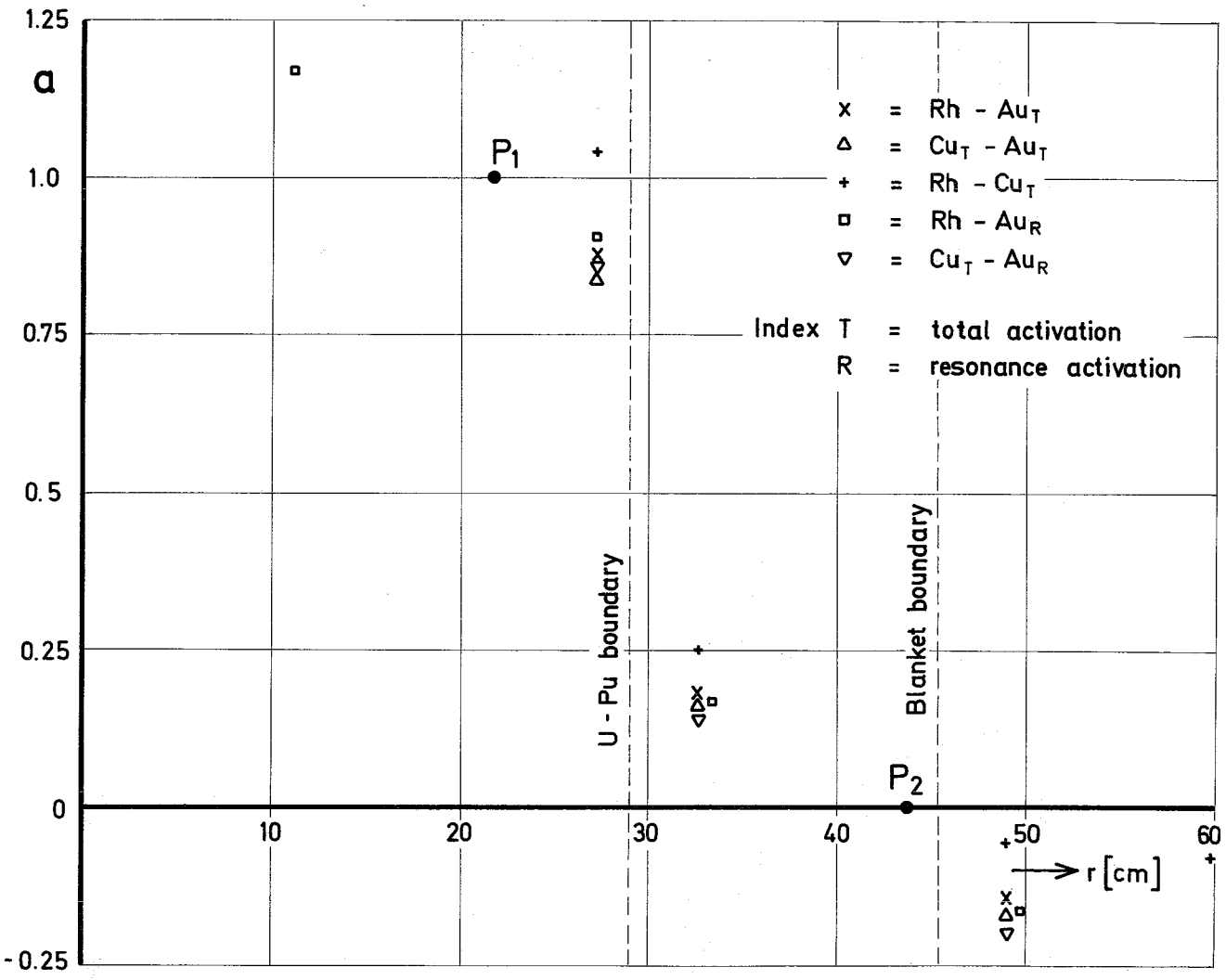

Fig. 7 Coefficients for Flux Synthesis

Radius of Pu - Zone = 29.9 cm

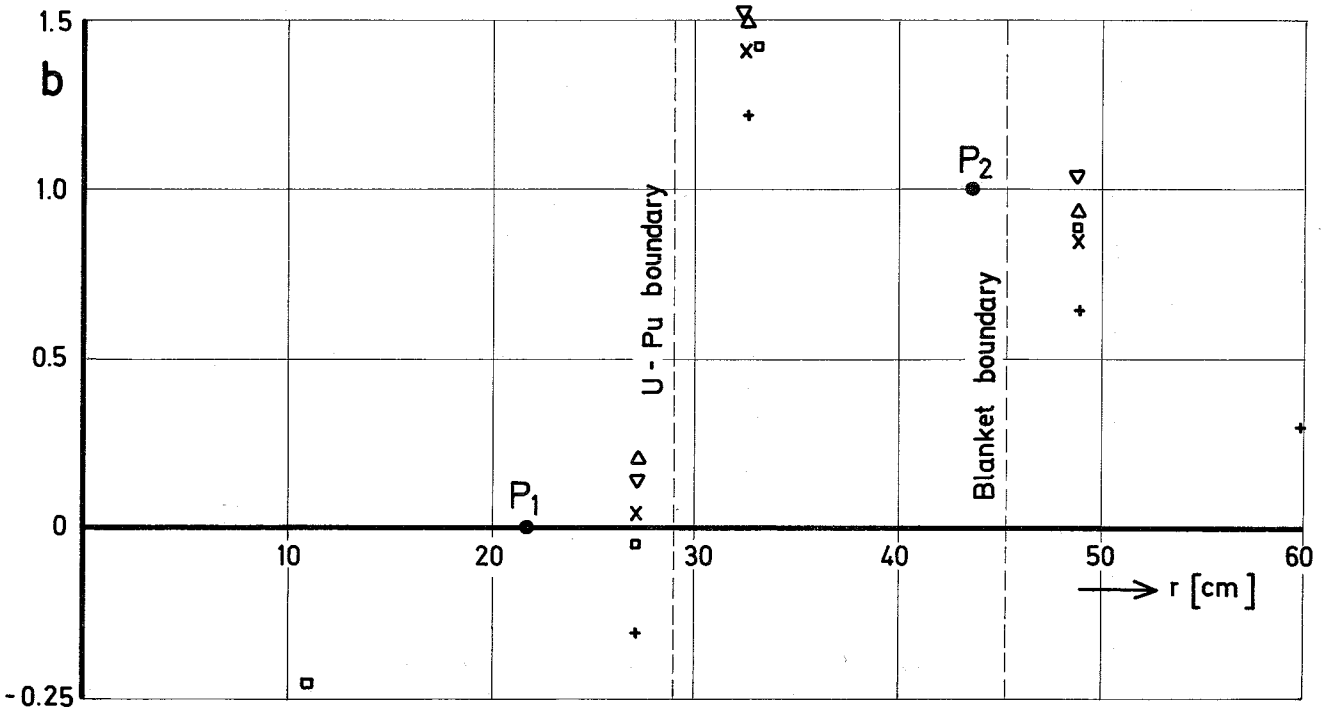

Fig. 8 Resonance Activation Au and Cu

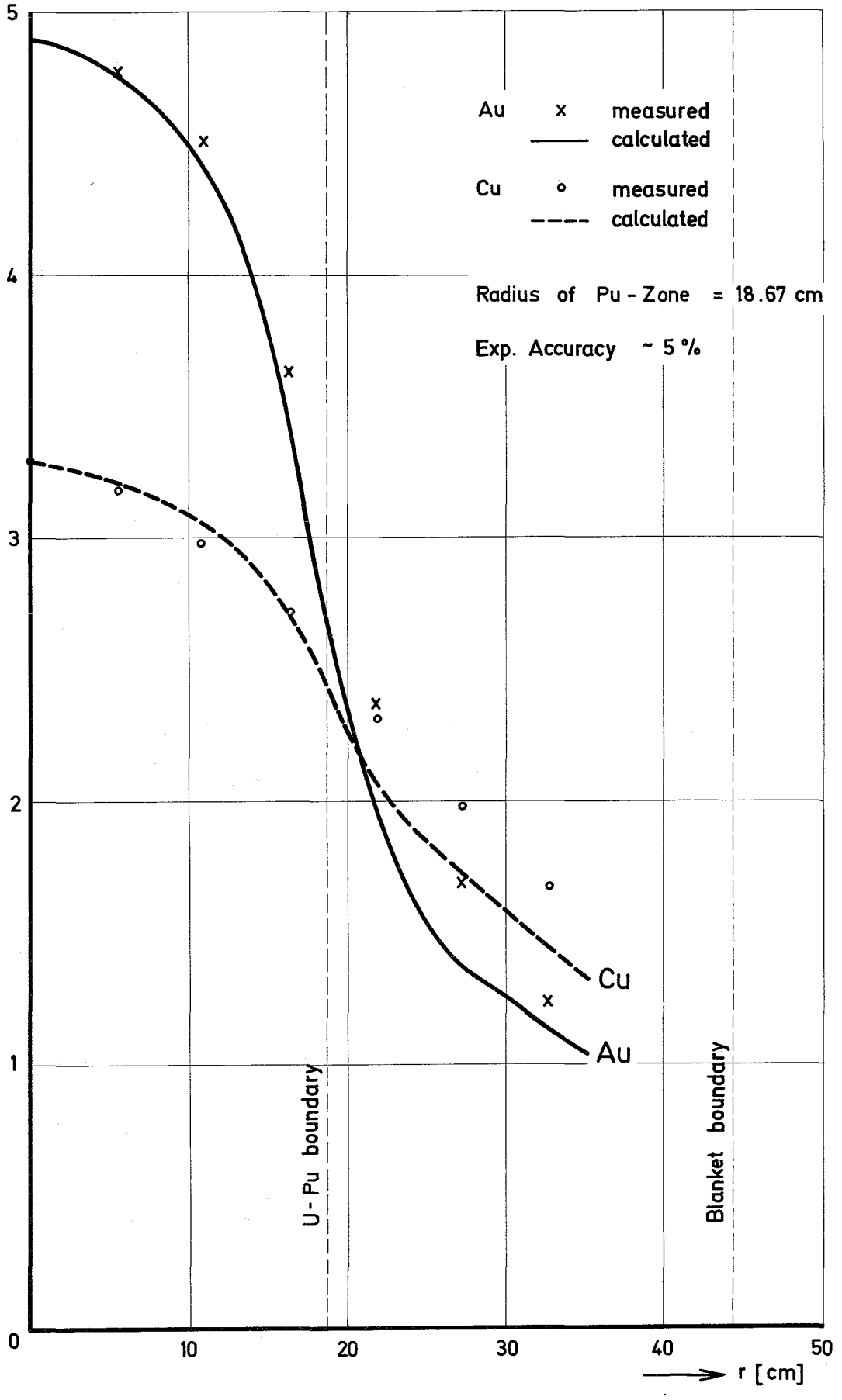

Fig. 9 Resonance Activation Au and Cu

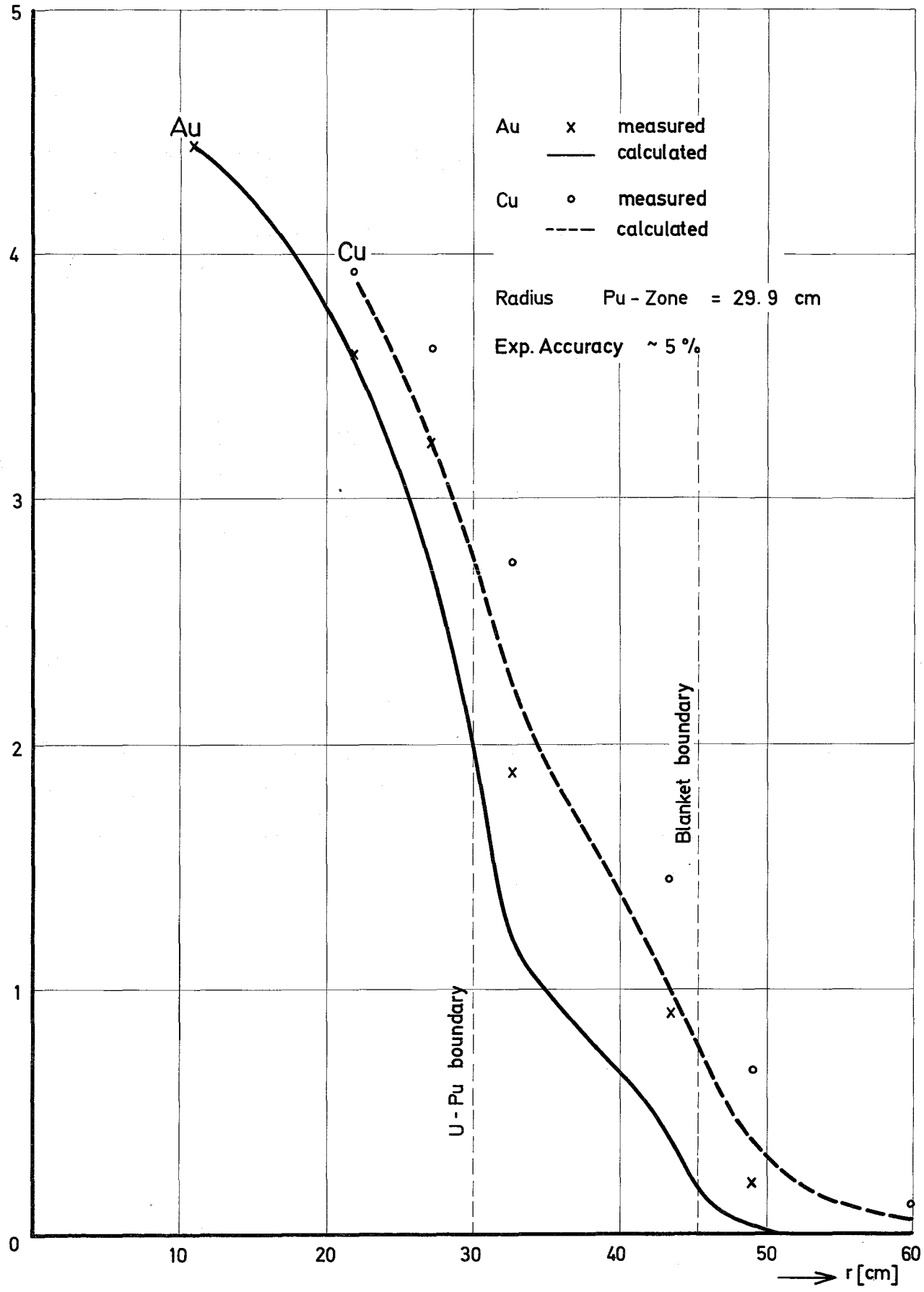

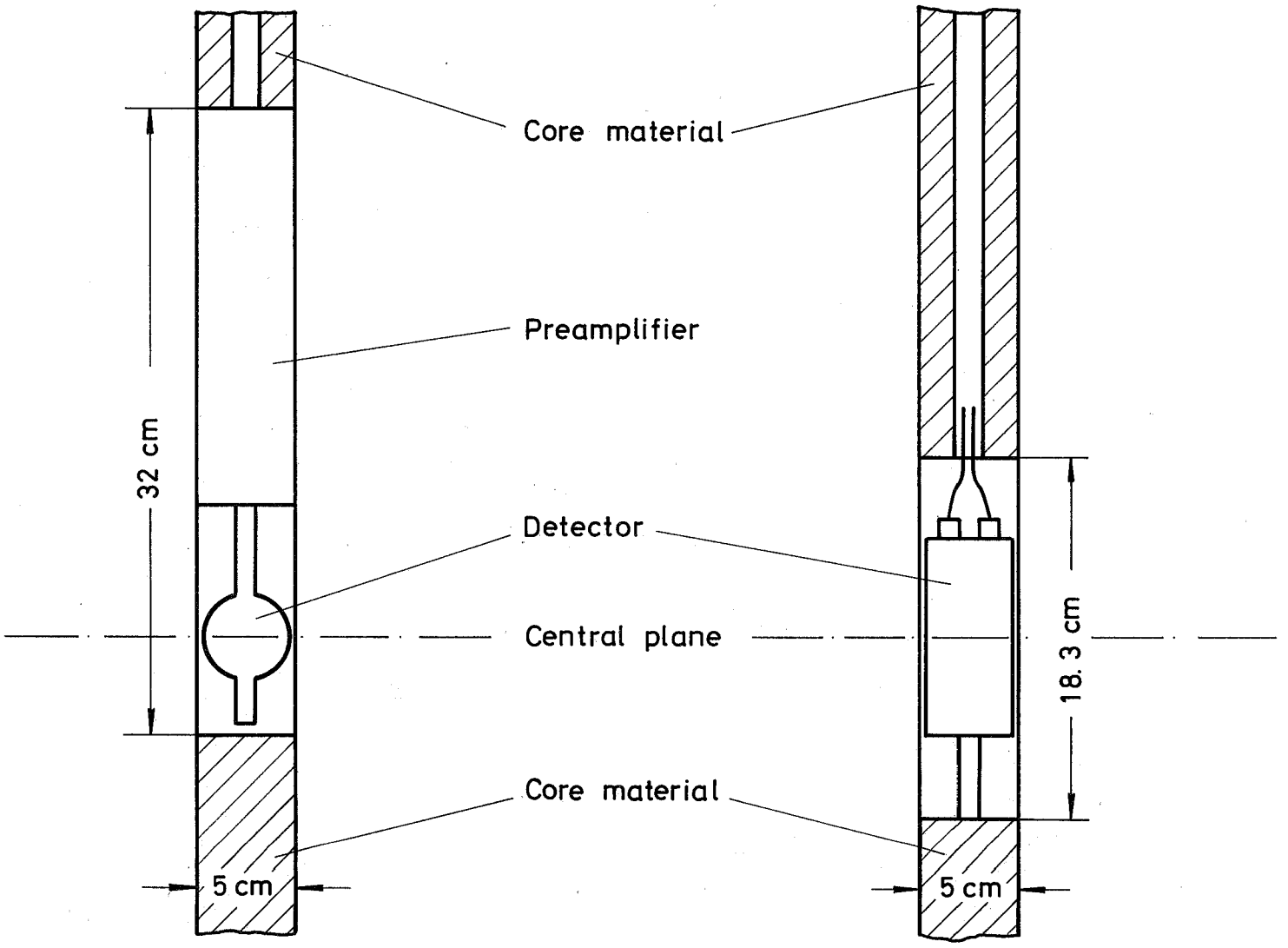

Fig. 10 Detector Subassemblies

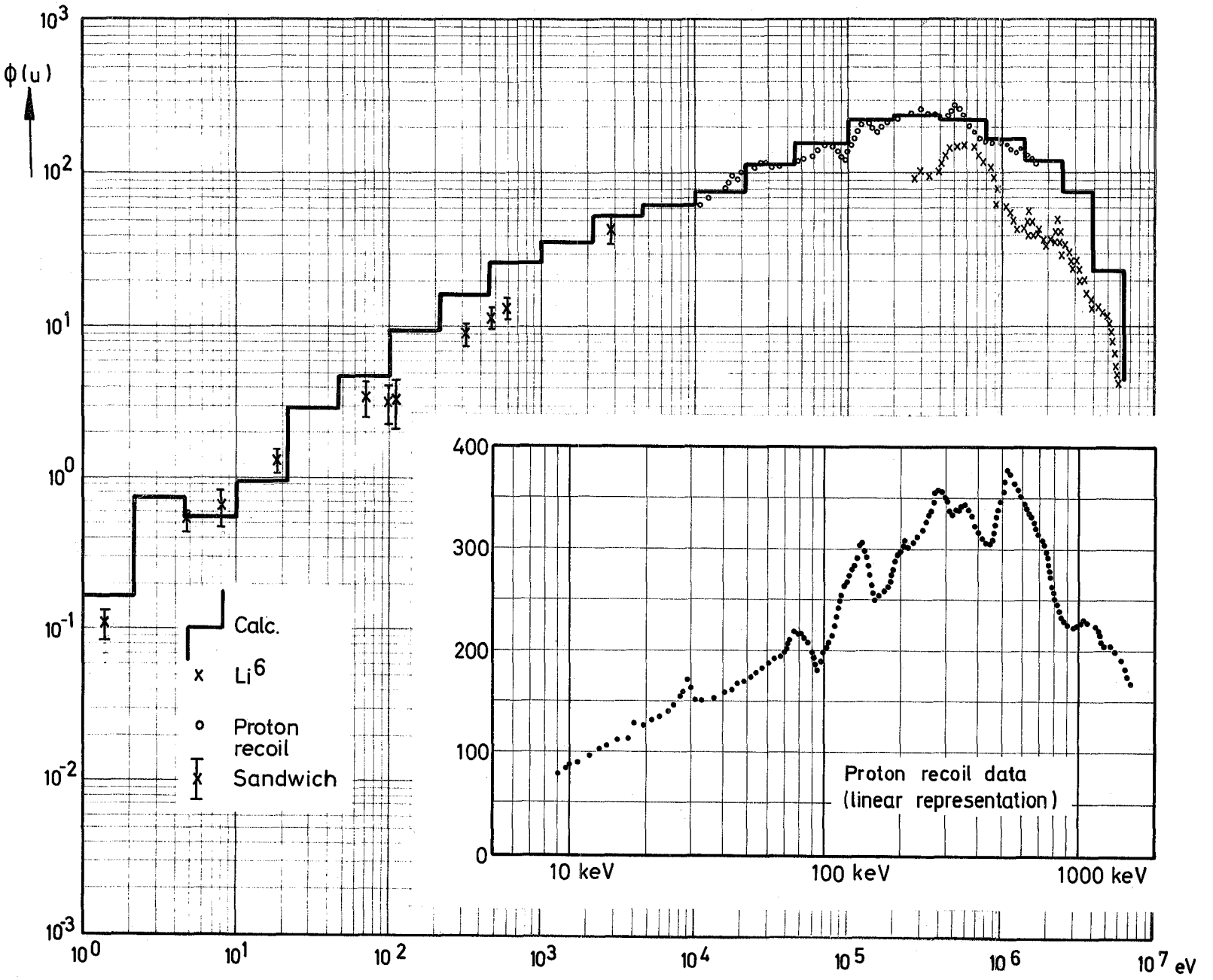

Fig. 11 Measured and calculated spectrum for SNEAK 3B-2

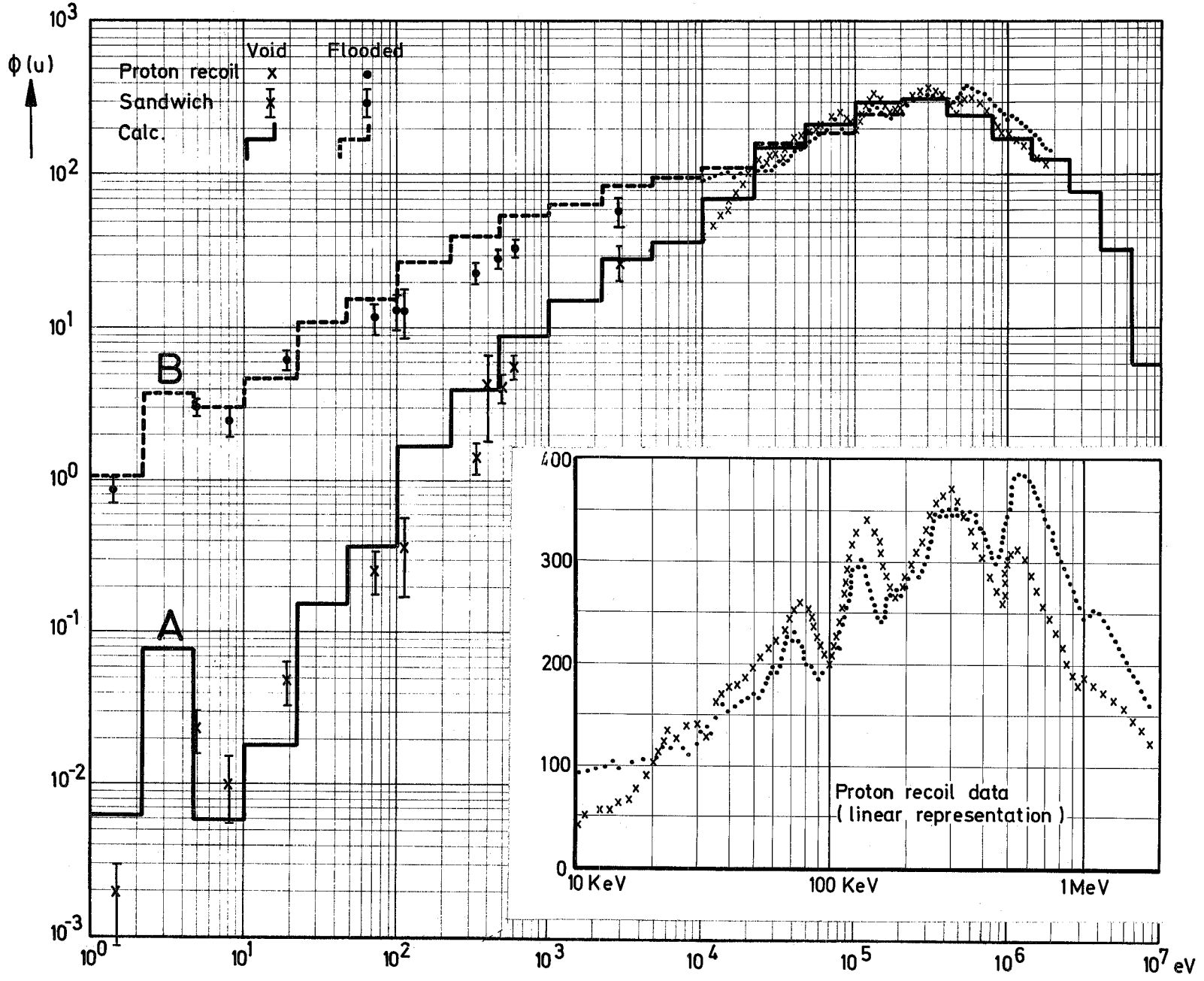

Fig. 12 Measured and calculated spectrum in SNEAK 3B - Void (A) and SNEAK 3B - Flooded (B)

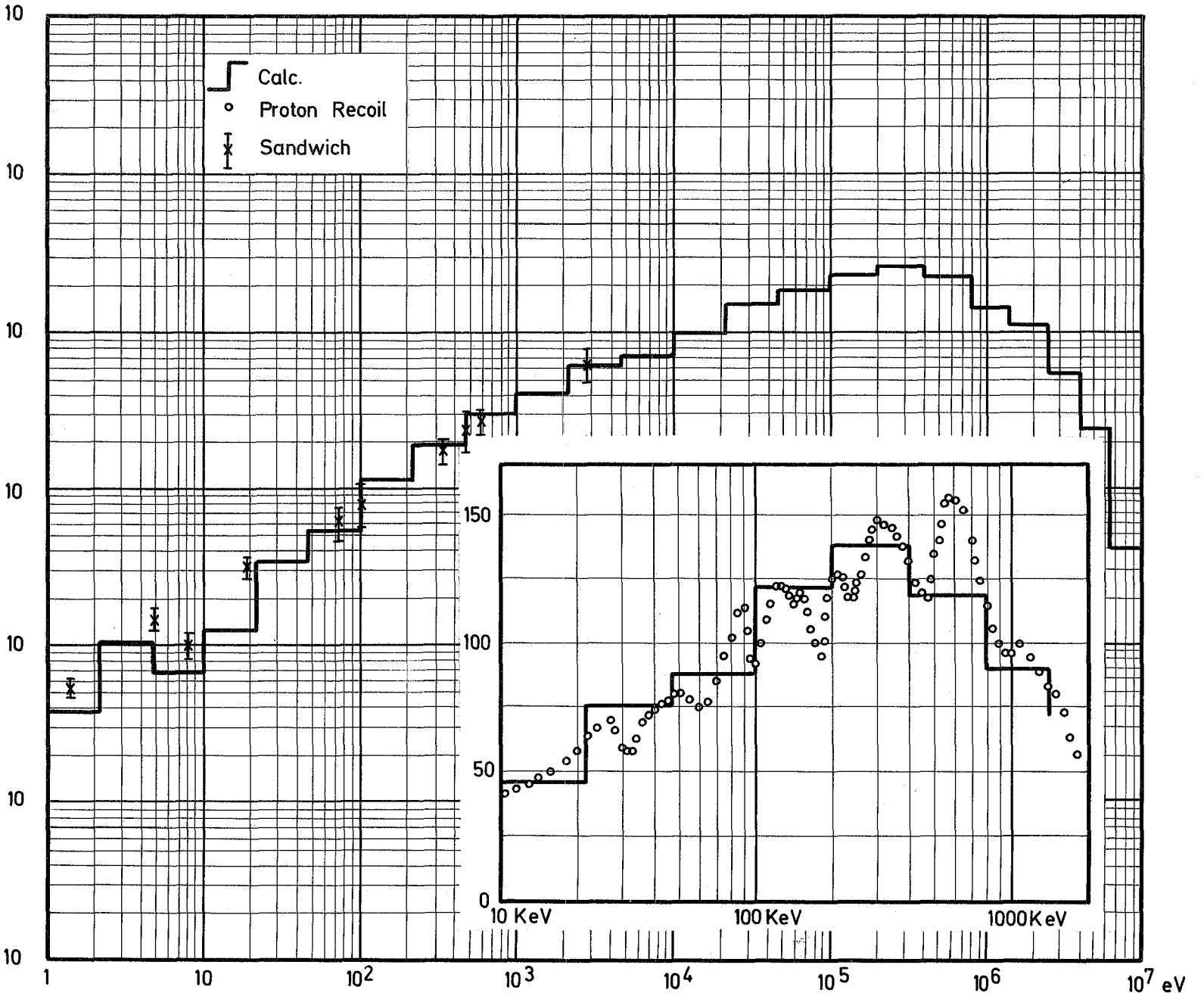

Fig. 13 Measured and calculated Spectrum in Assembly 3B - 2S

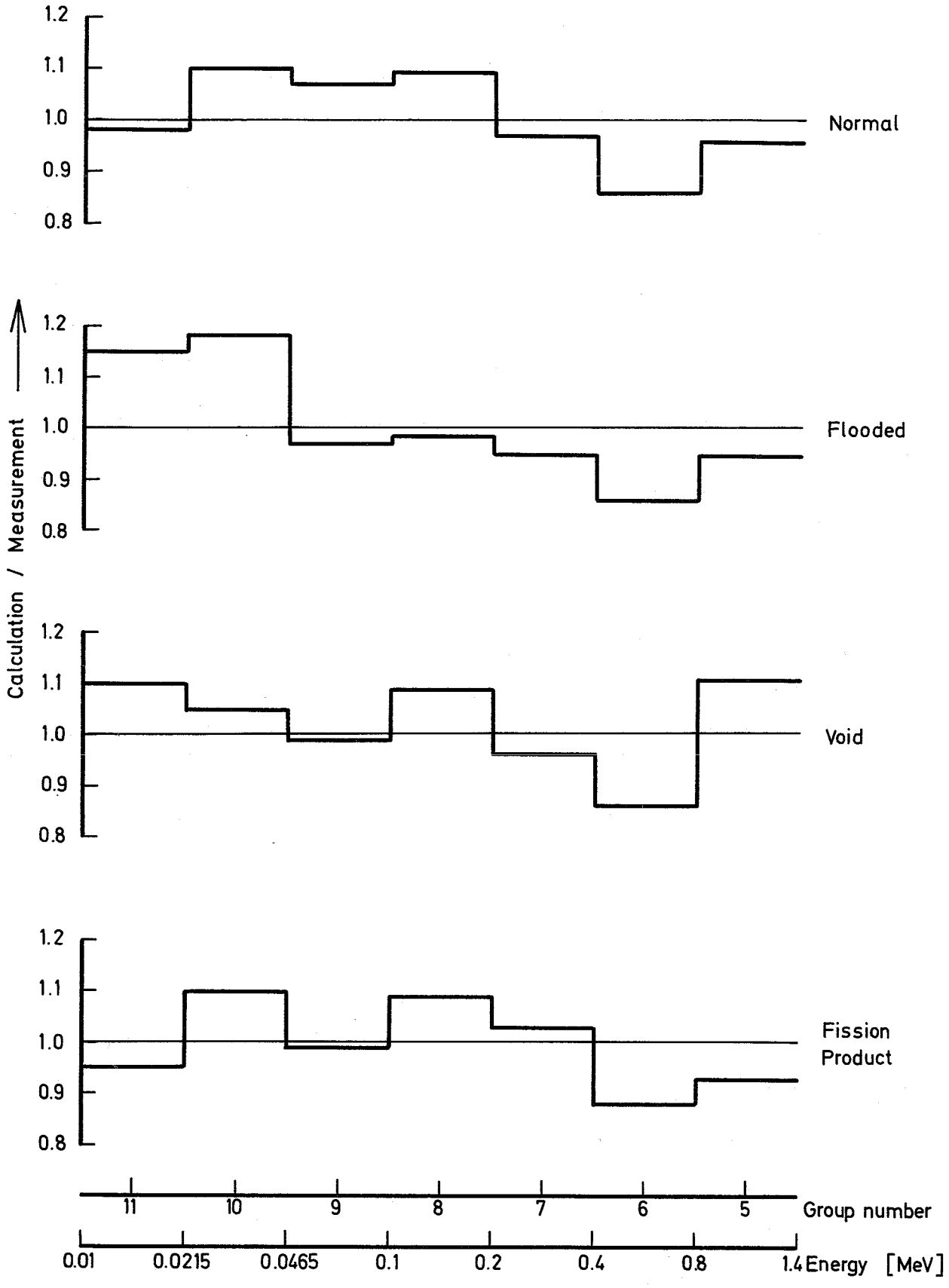

Fig. 14 Comparison of measured (Proton - Recoil) and calculated Neutron Spectra in the Center of SNEAK 3B - 2

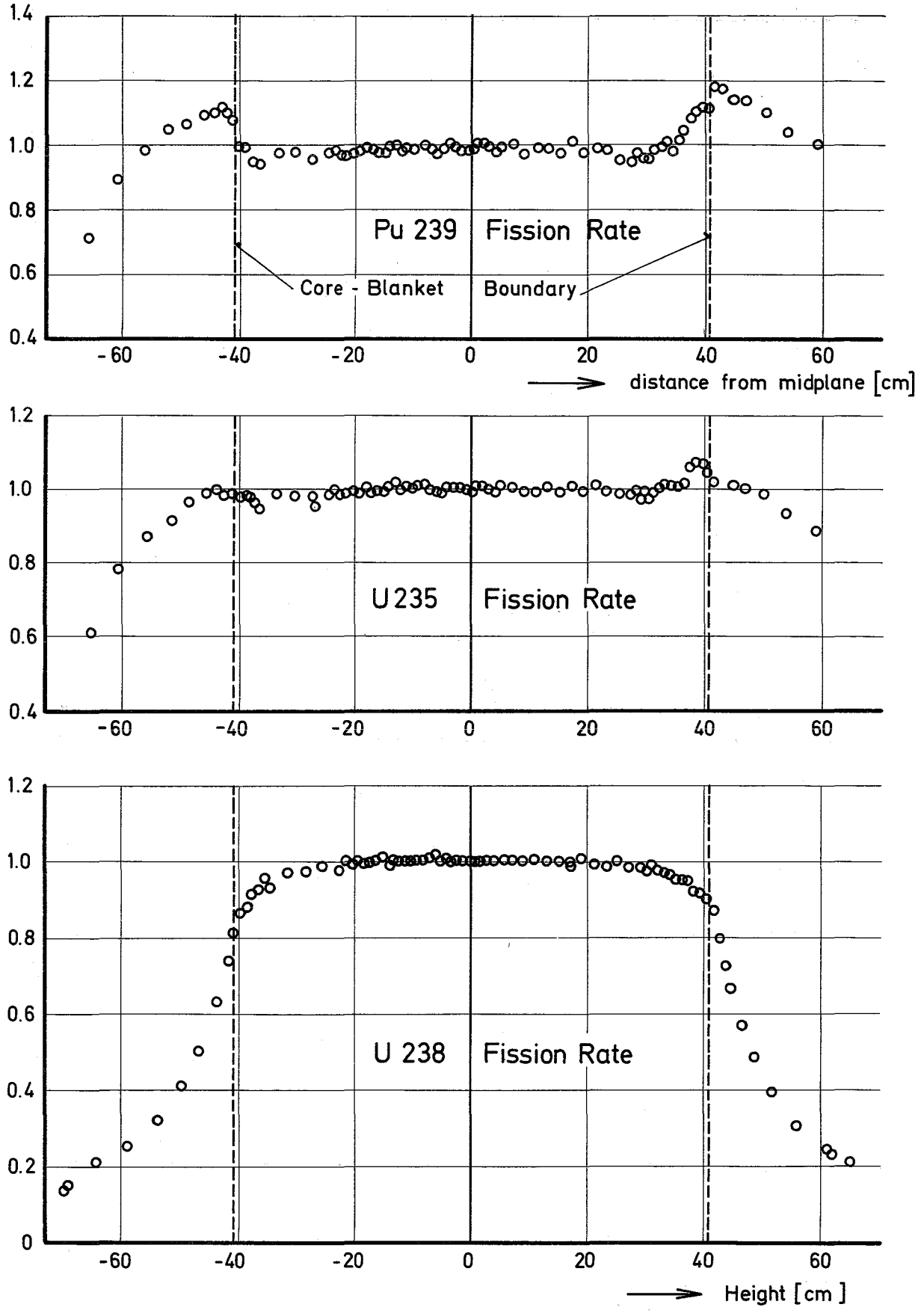

Fig. 15 Ratio of calculated to experimental Central axial Fission Rates of Pu 239, U 235 and U 238 (normalized at the Center) for SNEAK-Assembly 3B-2 (Chamber Traverses)

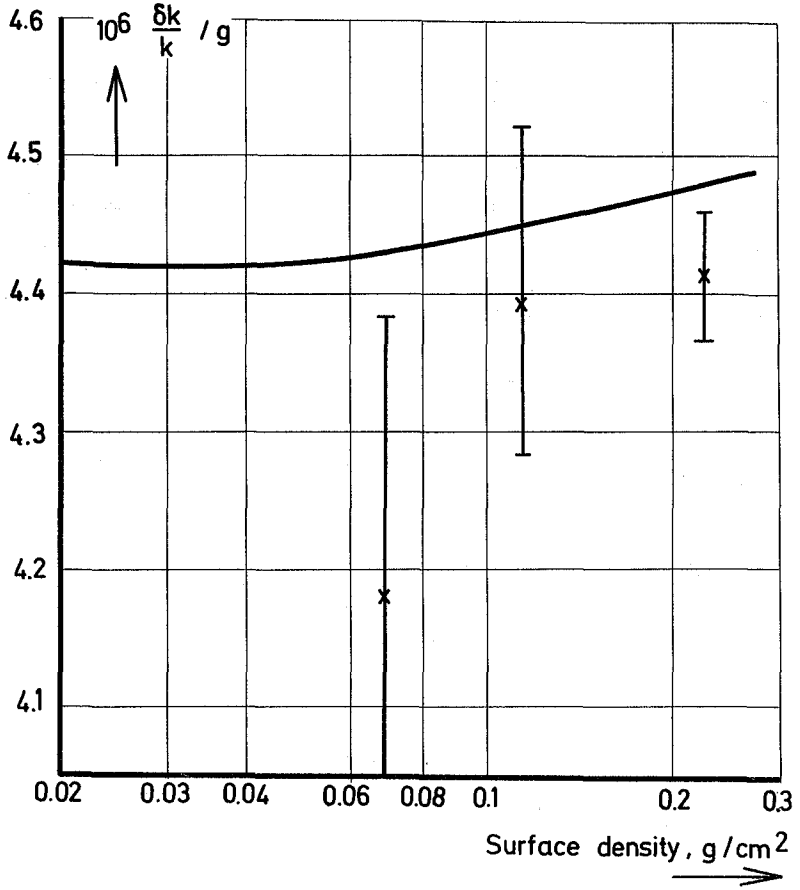

Material worth of Pu

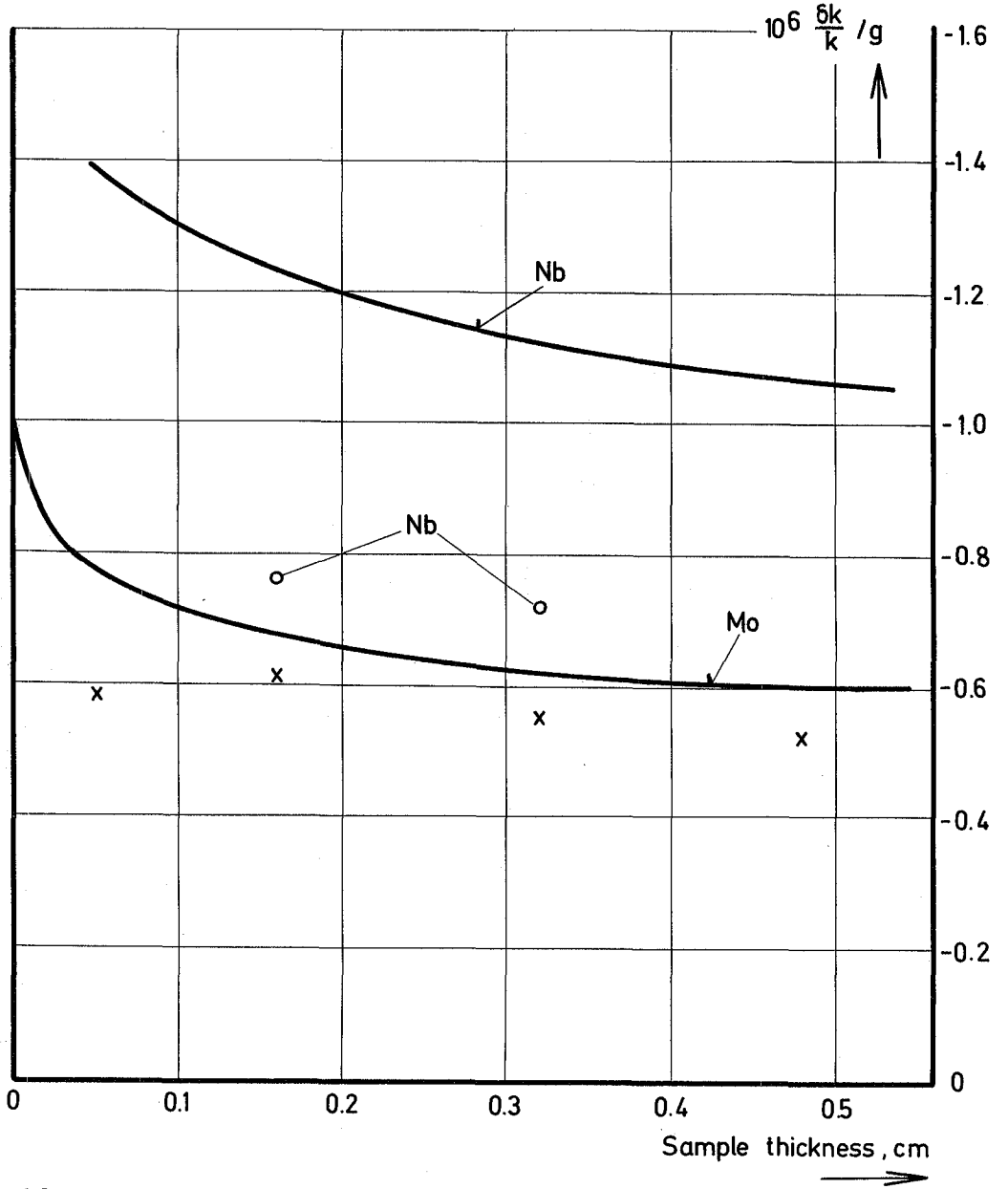

Material worth of Nb and Mo

Fig. 16

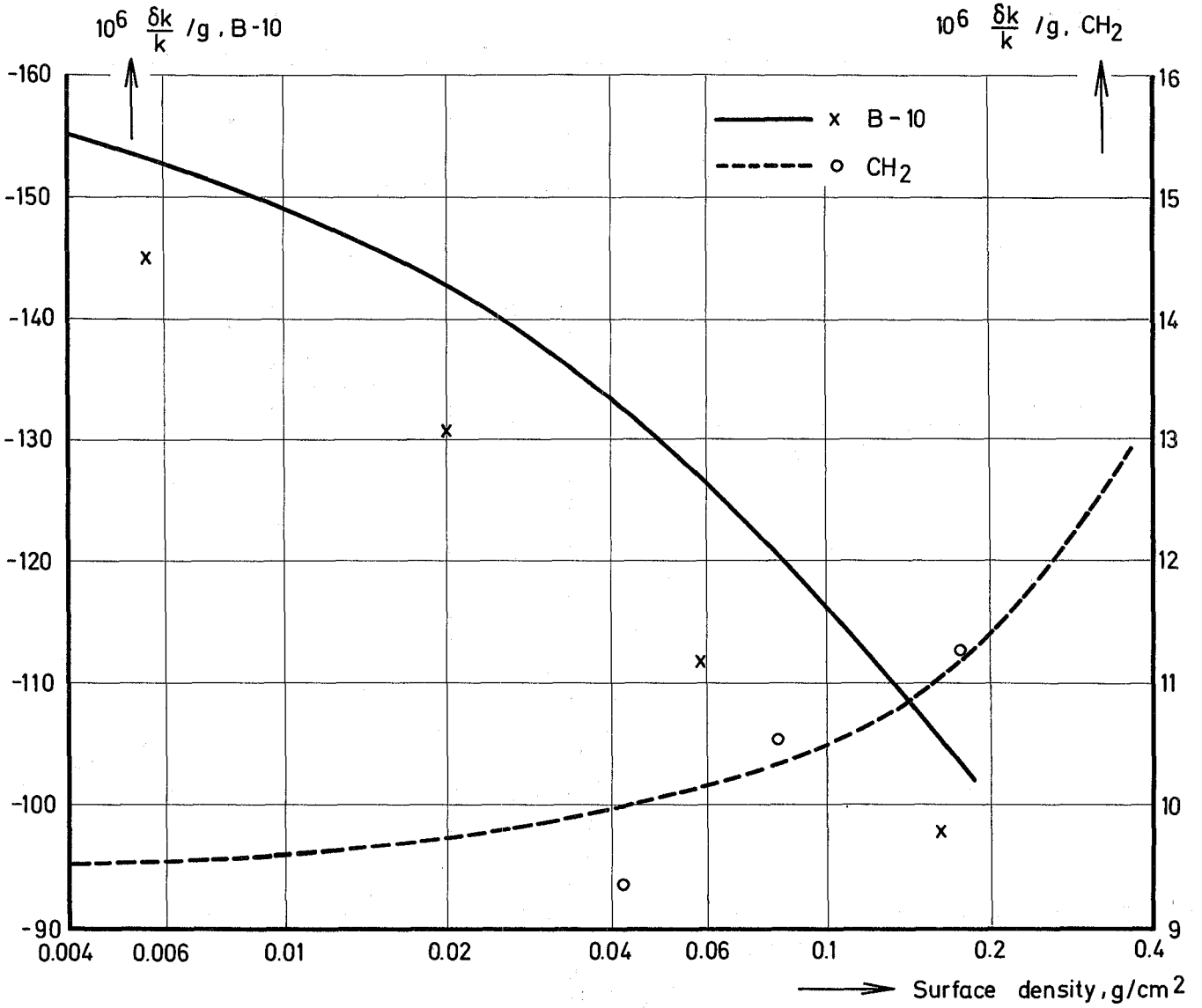

Fig. 17 SNEAK 3B-2 Material worth of B-10 and CH_2

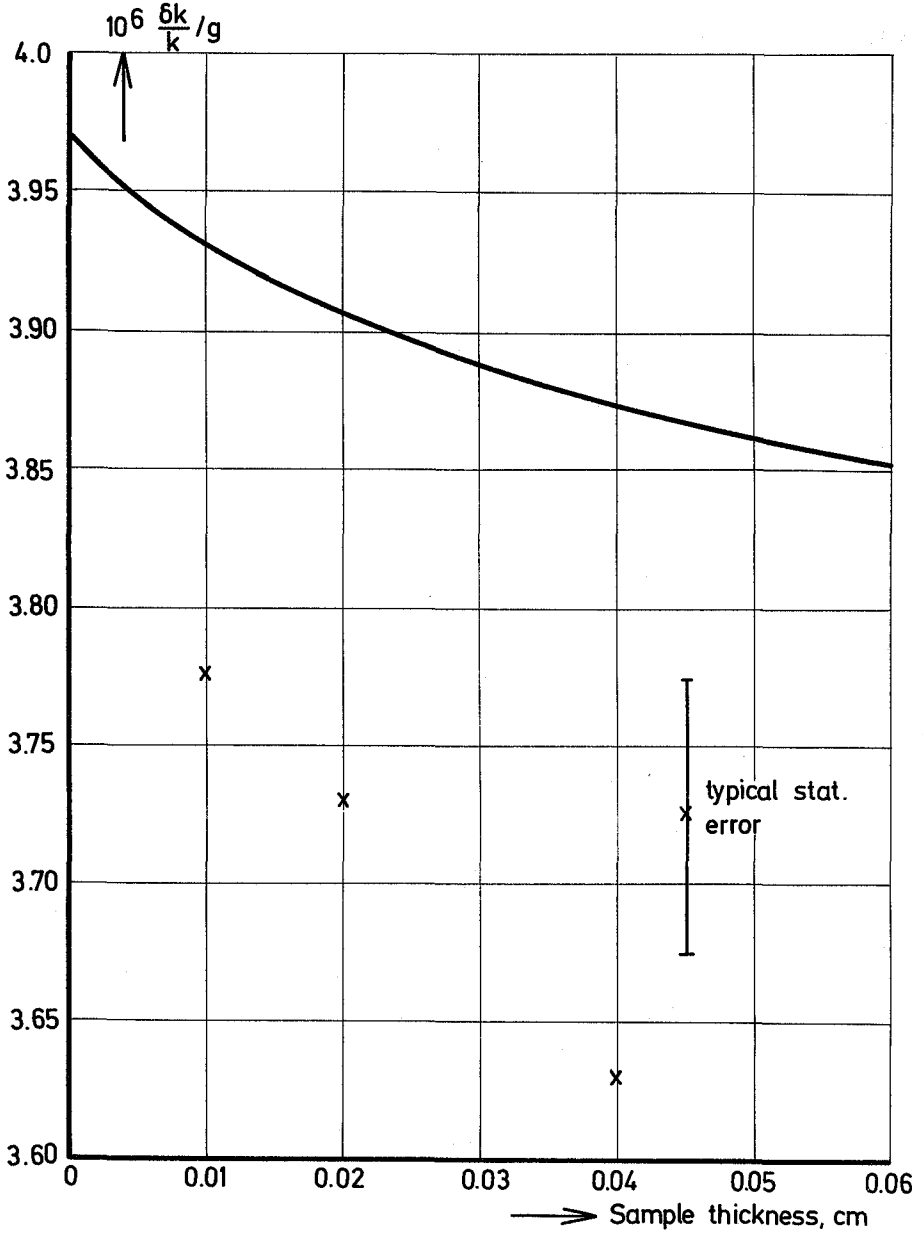

SNEAK 3B-2 Material worth of U 235

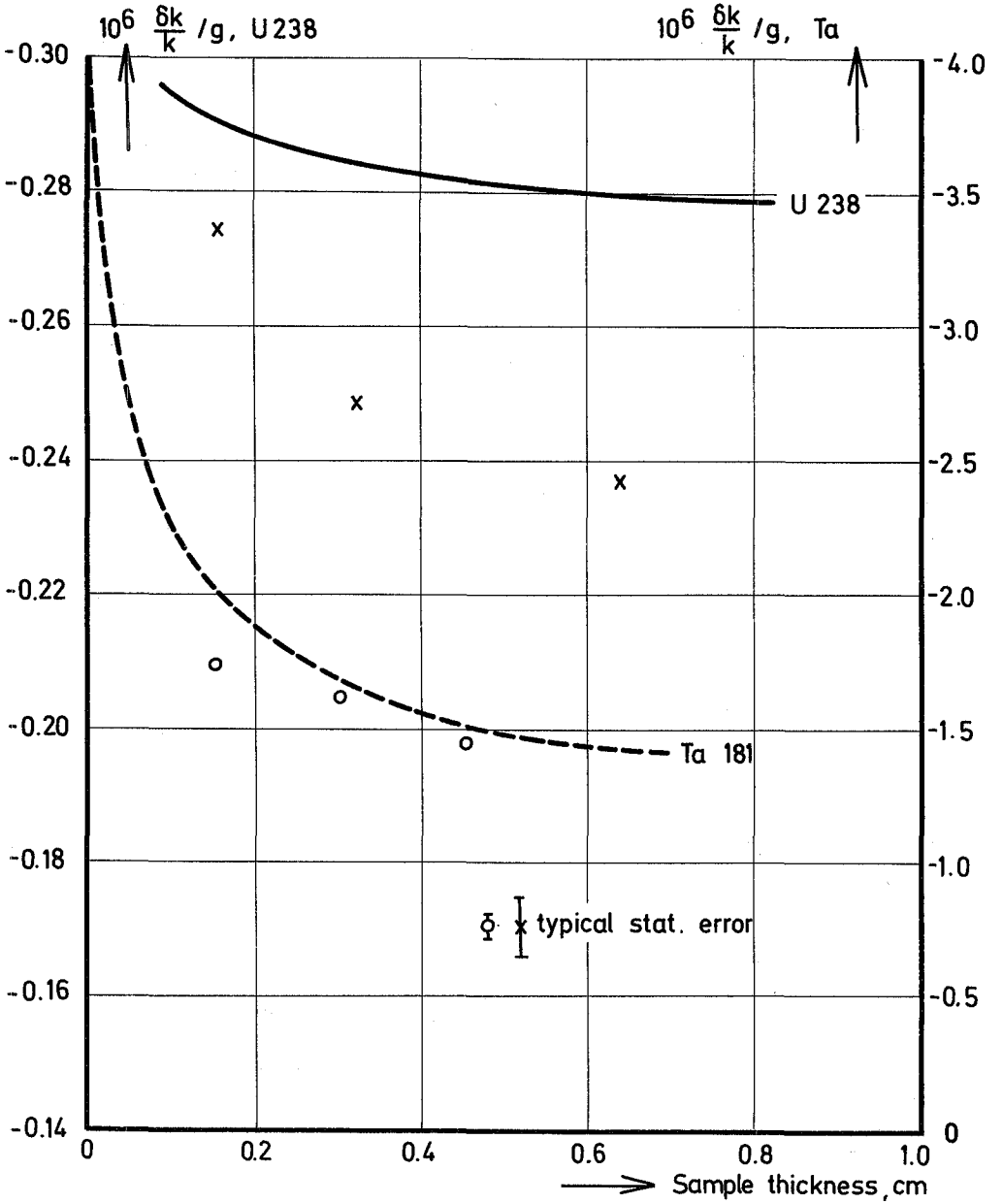

Fig. 18 Material worth of U238 and Ta

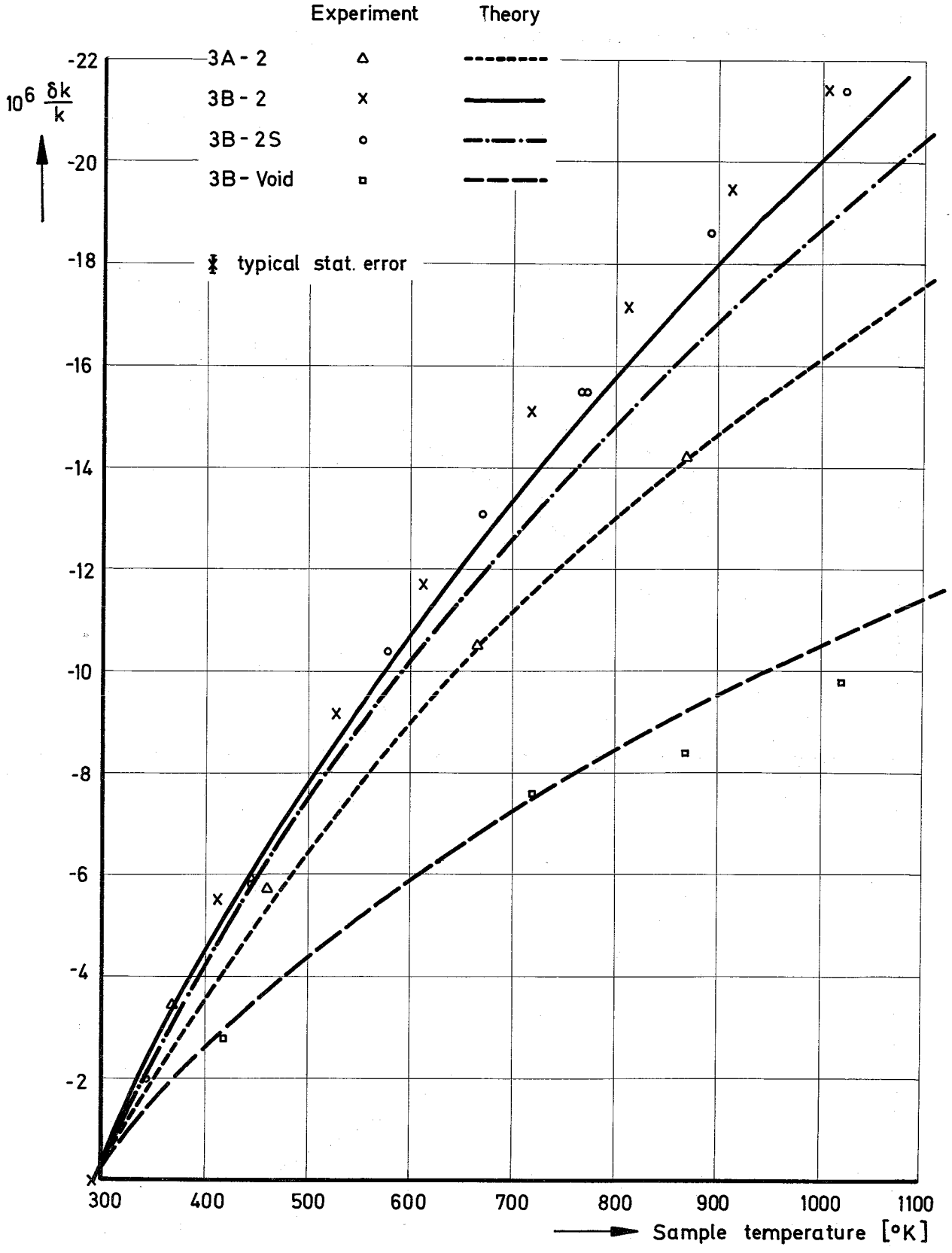

Fig. 19 Doppler reactivity measurements with a depleted UO_2 sample in SNEAK - 3

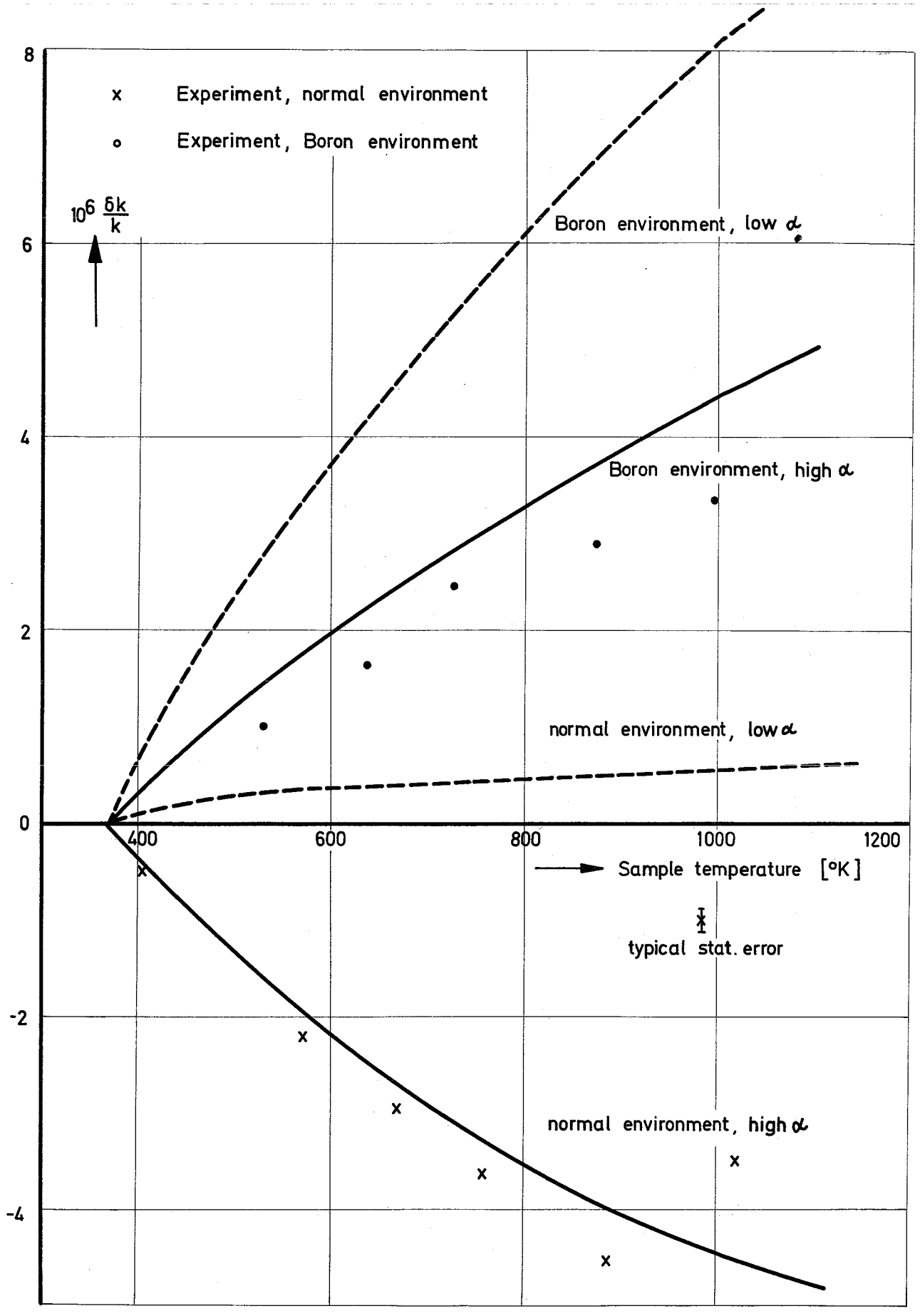

Fig. 20 Doppler reactivity measurements with PuO_2 sample (451.7 g) in SNEAK 3B-2

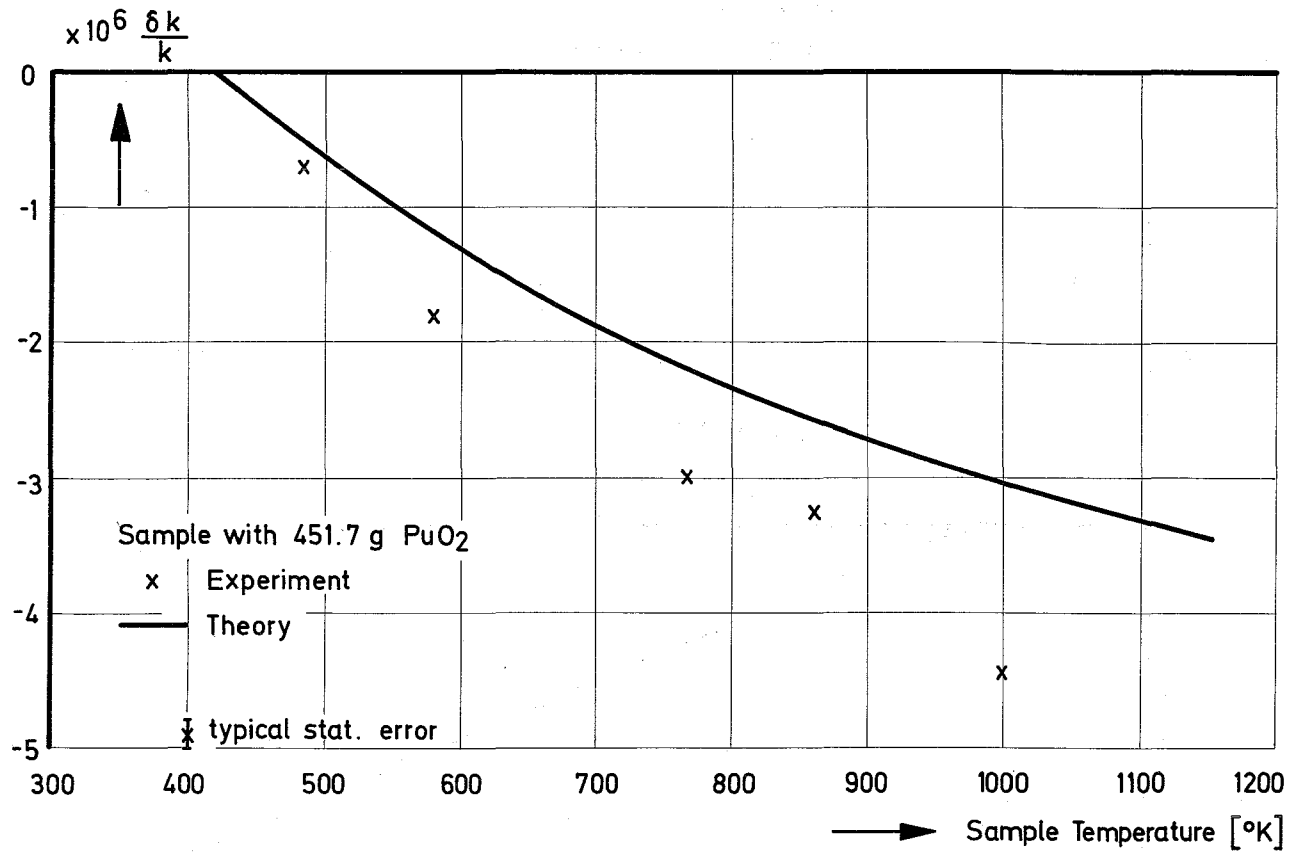

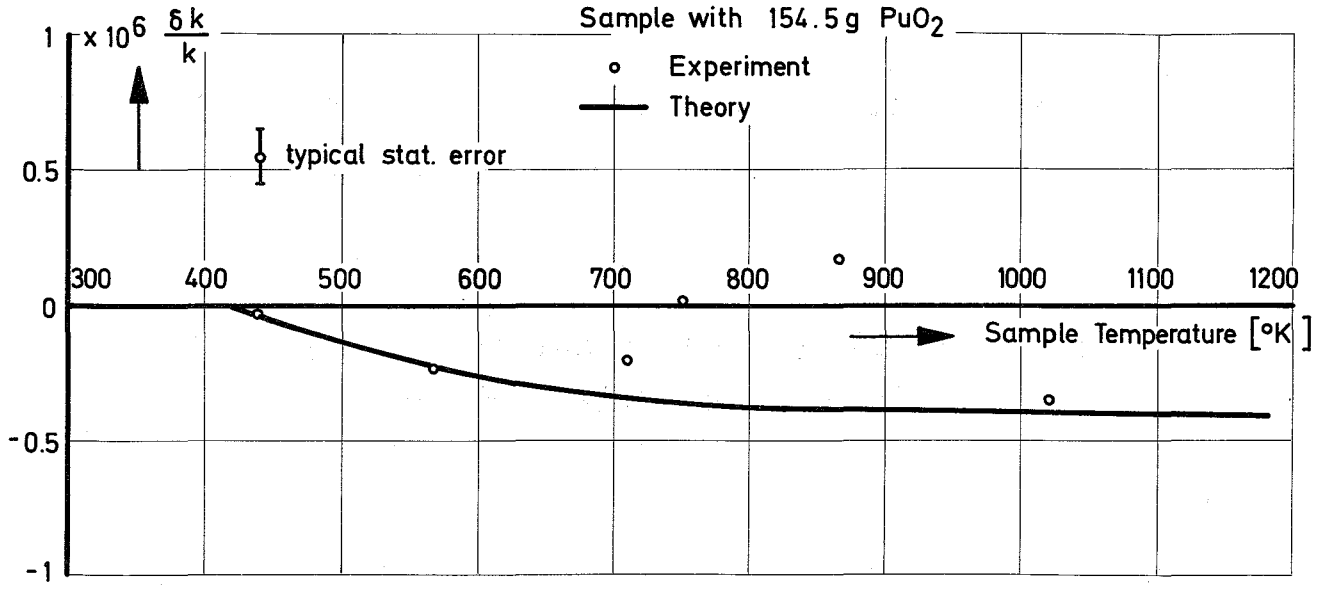

Fig. 21 Doppler Reactivity Measurements with PuO_2 - Samples in a Boron Environment designed to remove the overlap effect. SNEAK 3B-2

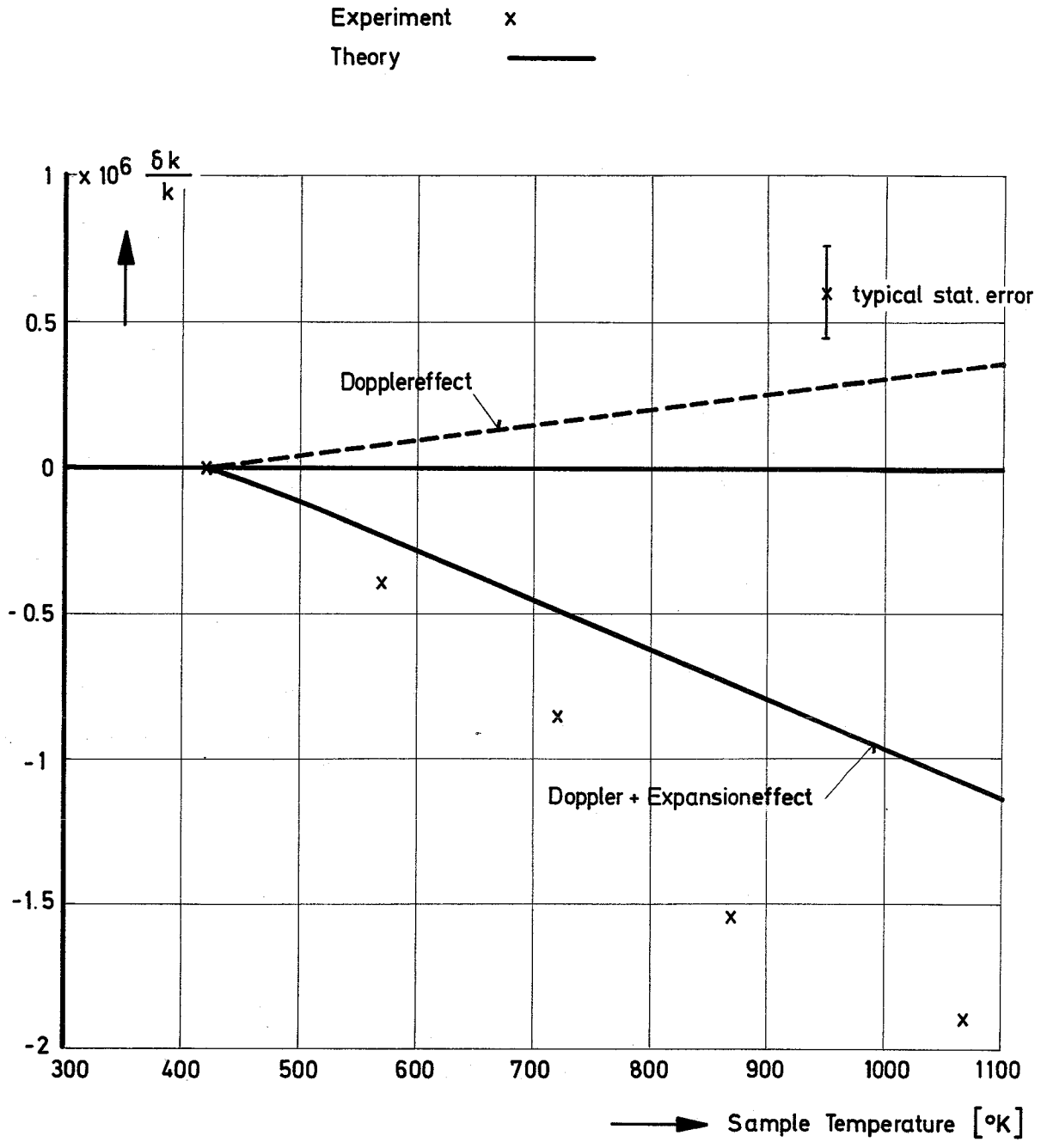

Fig. 22 Doppler Reactivity Measurements with a PuO_2 - Sample (451.7 g) in SNEAK 3B - Void

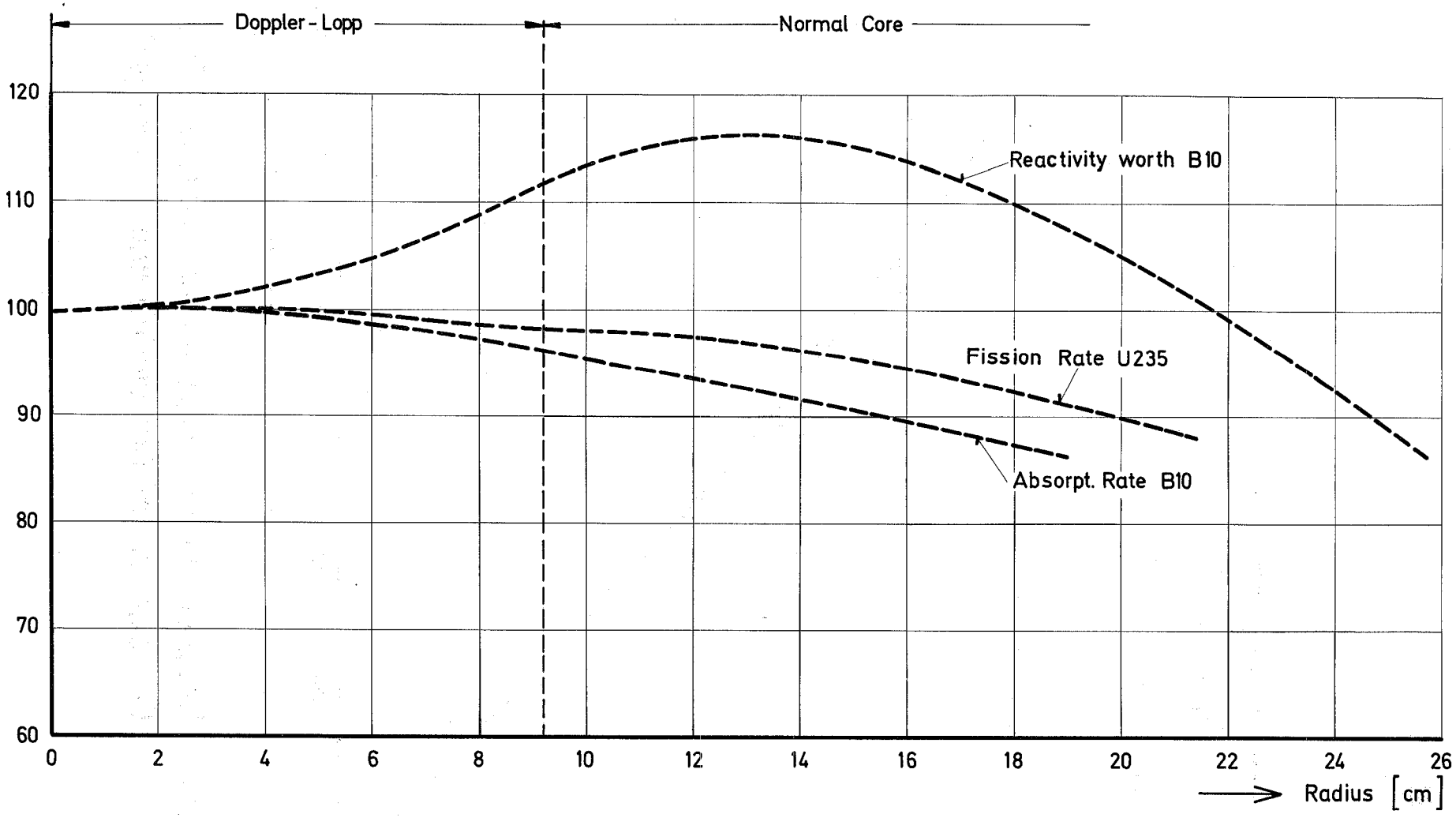

Fig. 23 Some Characteristics of Assembly 3B-2 with the Doppler-Loop Installed

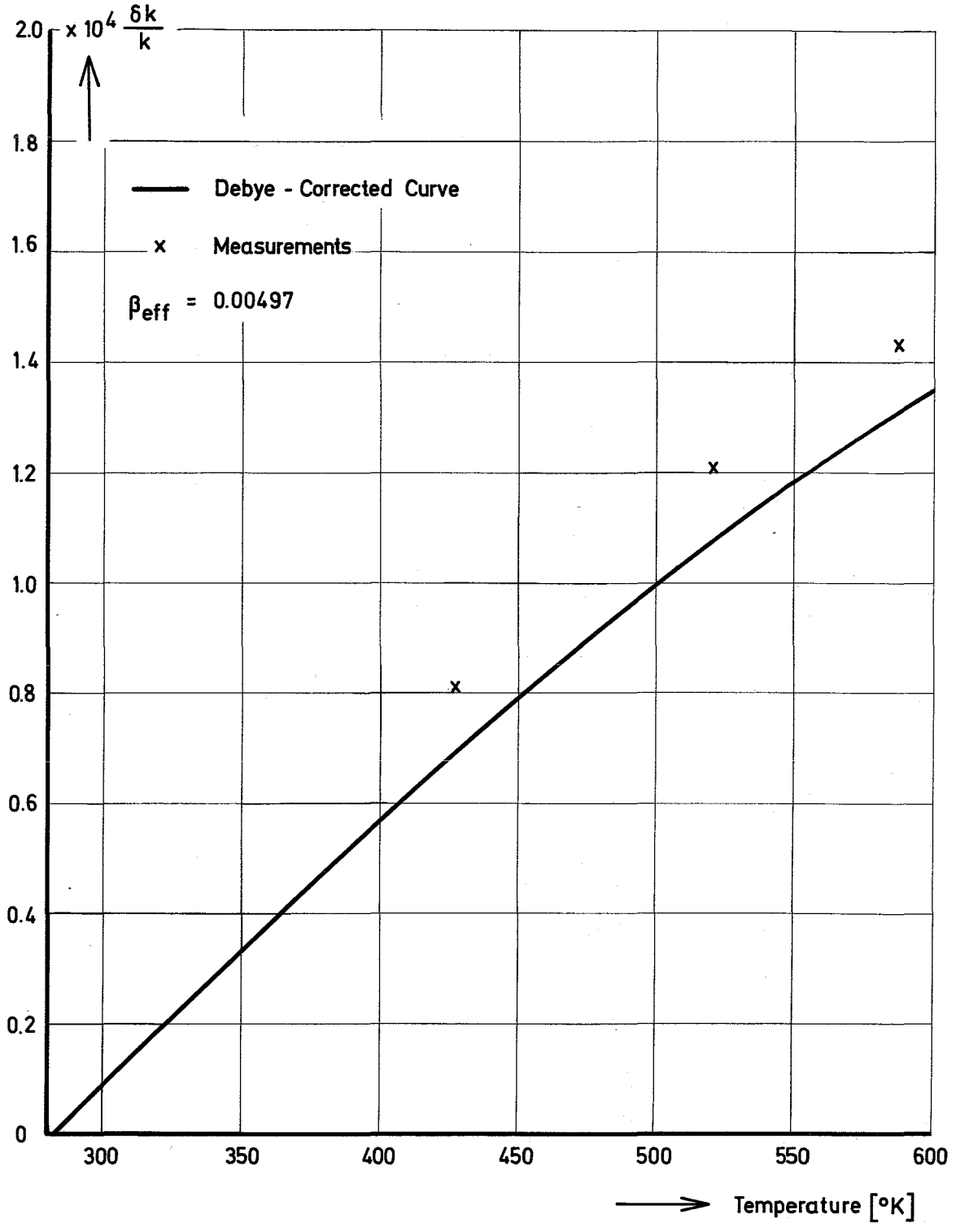

Fig. 24 Doppler - Loop - Experiment SNEAK 3B-2
Comparison of Calculation and Experiment

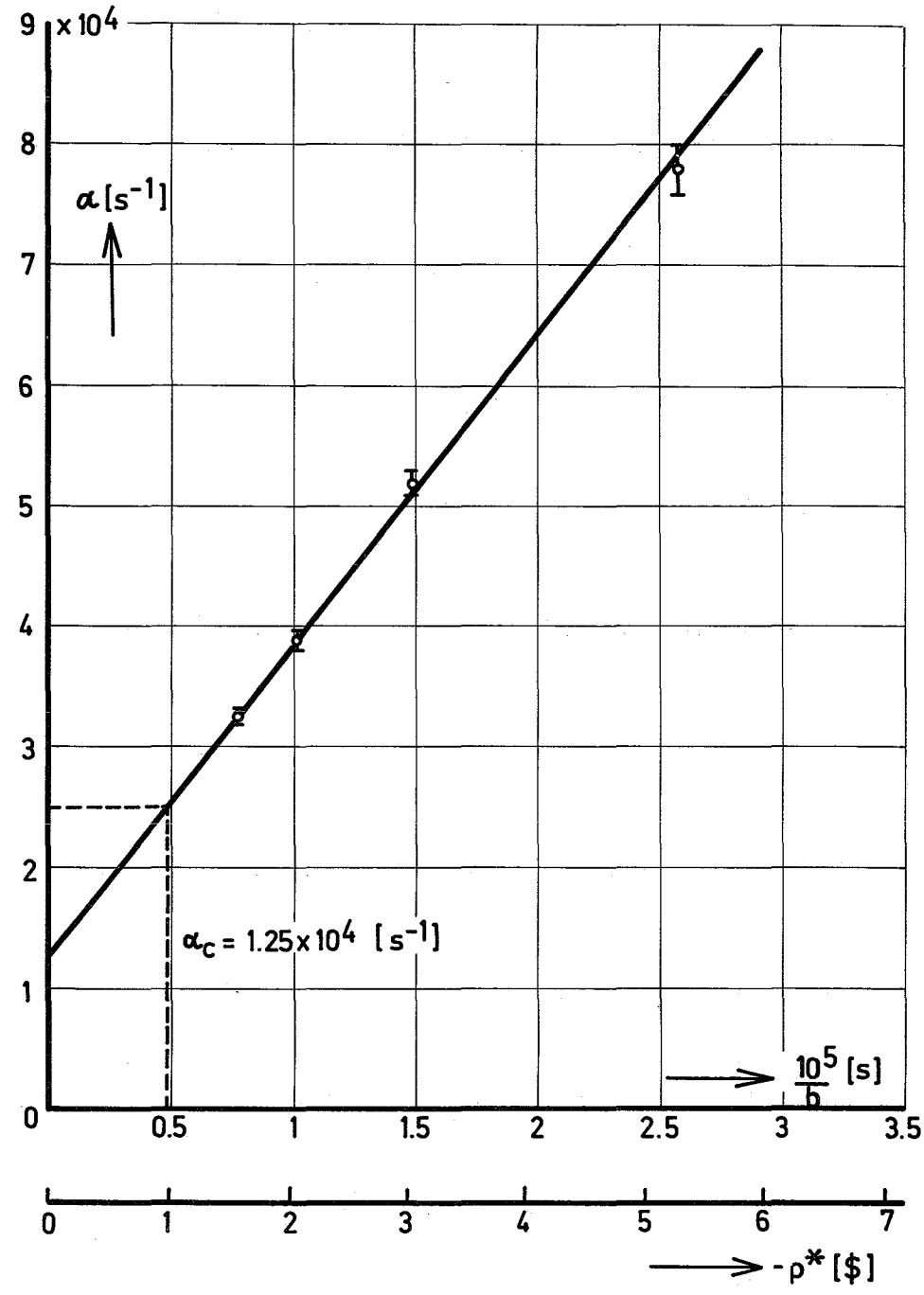

Fig. 25 Measured Rossi - α as a Function of the inverse Counting Rate 1/b and resulting Reactivity Calibration